Max Vogi, BSc

Performance of triethylene glycol as entrainer for the separation of the 1-propanol - water azeotrope: Measurements and modelling of vapor-liquid equilibria

Master Thesis

to achieve the university degree of
Diplom-Ingenieur
in
chemical and process engineering

submitted to
Graz University of Technology

Supervisor:
Assoc.Prof. Dipl.-Ing. Dr.techn. Thomas Wallek
Institute of Chemical Engineering and Environmental Technology

Co-Supervisor:
Dipl.-Ing. Maximilian Neubauer, BSc
Institute of Chemical Engineering and Environmental Technology

Graz, Oktober 2022

Graz University of Technology
Institute of Chemical Engineering and Environmental Technology

Performance of triethylene glycol as entrainer for the separation of the 1-propanol - water azeotrope: Measurements and modelling of vapor-liquid equilibria

Max Vogi, BSc
00373260

Graz, Oktober 2022

CEET
Chemical Engineering and Environmental Technology

AFFIDAVIT

I declare that I have authored this thesis independently, that I have not used other than the declared sources/resources, and that I have explicitly indicated all material which has been quoted either literally or by content from the sources used. The text document uploaded to TUGRAZonline is identical to the present master thesis.

Graz: _____ _____

(Signature)

Acknowledgement

An dieser Stelle möchte ich mich bei den Betreuern meiner Arbeit, Assoc.Prof. Dipl.-Ing. Dr.techn. Thomas Wallek und Dipl.-Ing. Maximilian Neubauer bedanken, die mich in der Erstellung meiner Arbeit unterstützt haben. Mein Dank gilt besonders Maximilian Neubauer, sowohl für die tatkräftige Unterstützung im Labor, als auch für die gute tägliche Zusammenarbeit im Büro. Mein Dank gilt auch Gallus Fleisch für seine zuverlässige Arbeit im Labor.

Des Weiteren möchte ich mich bei meiner Familie bedanken, die mich über den gesamten Verlauf des Studiums, sowie auch im Rest meines Lebens immer tatkräftig unterstützen.

Abstract

For the separation of the 1-propanol-water azeotrope, a well suited entrainer is to be found. For this purpose, several entrainer candidates are first compared in their selectivity, after which the choice falls on triethylene glycol. To allow a more in-depth analysis of the behaviour of the ternary system of triethylene glycol, 1-propanol and water, a parameterized thermodynamic model is needed. For this purpose, experiments are carried out with all binary subsystems and a vapour-liquid equilibrium data set is compiled. From this data set, as well as literature data on activity coefficients at infinite dilution, the binary interaction parameters for the non random two liquid (NRTL) model are regressed. The ability of these parameters to correctly represent the ternary system is checked by comparison with an experimentally determined data set. Since the parity of the measured data and the model behaviour is satisfactory, the model is used to represent the dependence of the relative volatility of the azeotropic mixture on the proportion of triethylene glycol in the mixture. For breaking the 1-propanol - water azeotrope, a minimum entrainer mole fraction of $0.515\left[\frac{\mathrm{mol_{TEG}}}{\mathrm{mol}}\right]$ was determined, corresponding to a mass fraction of $0.727\left[\frac{\mathrm{kg_{TEG}}}{\mathrm{kg}}\right]$.

Kurzfassung

Für die Trennung des 1-Propanol-Wasser-Azeotrops soll ein effektiver Entrainer gefunden werden. Dazu werden zuerst mehrere Entrainer-Kandidaten in ihrer Selektivität verglichen, wonach die Wahl auf Triethylenglycol fällt. Um das Verhalten des ternären Systems aus Triethylenglykol, 1-Propanol und Wasser eingehender analysieren zu können, wird ein parametrisiertes thermodynamisches Modell benötigt. Dazu werden Versuche mit allen binären Teilsystemen durchgeführt, und ein Dampf-Flüssig Gleichgewichtsdatensatz zusammengestellt. Aus diesem Datensatz, sowie Literaturdaten zu Aktivitätskoeffizienten bei unendlicher Verdünnung, werden die binären Wechselwirkungsparameter für das non-random two liquid (NRTL) Model regressiert. Die Fähigkeit dieser Parameter, das ternäre System richtig abzubilden wird überprüft durch einen Vergleich mit einem experimentell bestimmten Datensatz. Da die Parität der Messdaten und des Modellverhaltens zufriedenstellend ist, wird das Modell verwendet, um die Abhängigkeit der relativen Flüchtigkeit des azeotropen Gemischs von dem Anteil des Triethylenglycols in der Mischung darzustellen. Zur Auflösung des 1-Propanol - Wasser Azeotrops wurde ein minimaler Entrainer-Molanteil von $0.515\left[\frac{\mathrm{mol_{TEG}}}{\mathrm{mol}}\right]$ ermittelt, das entspricht einem Massenanteil von $0.727\left[\frac{\mathrm{kg_{TEG}}}{\mathrm{kg}}\right]$.

Contents

AFFIDAVIT III

Acknowledgement IV

Abstract V

Kurzfassung VI

List of Symbols and Abbreviations IX

List of Figures XI

List of Tables XIII

1 Introduction 1

2 Theoretical Background 2
2.1 Extractive Distillation . . . 2
2.2 Phase Equilibrium . . . 4
2.2.1 Vapor Liquid Equilibrium . . . 5
2.2.2 Mixing Enthalpy . . . 7
2.3 The Non-Random-Two-Liquid Model . . . 8
2.3.1 Fitting NRTL Model Parameters . . . 10
2.3.2 Activity Coefficients at Infinite Dilution . . . 10

3 Materials and Methods 12
3.1 Determination of Suitable Entrainers . . . 12
3.2 Laboratory Materials . . . 13
3.3 VLE Apparatus . . . 13
3.4 Analytics . . . 15
3.4.1 Density Measurement . . . 16
3.4.2 Karl Fischer Titration . . . 16
3.4.3 Gas Chromatography . . . 17

4 Data Processing and Calculations 19
4.1 Laboratory Data Processing . . . 19
4.1.1 Temperature and Pressure Data . . . 19
4.1.2 Composition Data . . . 20
4.2 Literature Data . . . 21
4.3 Material Properties . . . 21

4.4 Regression of model parameters 22
4.4.1 Objective Function 23
4.5 Parameter Validation 24
4.6 Entrainer Evaluation 25

5 Results and Discussion **26**
5.1 Experimental Data 26
5.2 Parameter Validation 29
5.3 Entrainer Evaluation 35

6 Summary and Outlook **39**

7 Bibliography **41**

8 Appendix **44**

List of Symbols and Abbreviations

Symbols

d	Total Differential
∂	Partial Differential
f	Fugacity
f_i^0	Standard Fugacity
g	Molar Gibbs Free Energy
$\overline{g_i}$	Partial Molar Gibbs Free Energy
h	Molar Enthalpy
k	Factor for Gas Chromatography Calibration
n	Amount of Substance
s	Molar Entropy
v_i^{L}	liquid molar volume
w	Weight Fraction
x	Liquid Phase Molar Fraction
y	Vapor Phase Molar Fraction
z	Molar Fraction
A	NRTL Binary Interaction Parameter
B	NRTL Binary Interaction Parameter
C	Entrainer Capacity
E	NRTL Binary Interaction Parameter
F	NRTL Binary Interaction Parameter
G	NRTL Model Parameter
MM	Molar Mass
Obj	Objective Function
P	Pressure
P^0	Standard Pressure
P_i^{s}	Vapor Pressure
Poy	Poynting Factor
R	Gas Constant
$RMSRD$	Root Mean Square Relative Deviation
S	Entrainer Selectivity
T	Temperature

Greek Symbols

α	Relative Volatility
α	NRTL Parameter / Non-randomness Factor
γ	Activity Coefficient
θ	Dimensionless Temperature
μ	Chemical Potential
ξ	Dimensionless Timescale
ρ	Density
τ	NRTL Parameter
ϕ	Fugacity Coefficient
ω	Weighting Factor
$\Delta\square$	Property Difference

Subscripts and Indices

$\square^{\infty}$	Property at Infinite Dilution
$\square^{0}$	Property at Standard Conditions
$\square_{i}$	Component Index
$\square_{j}$	Component Index
$\square_{n}$	Number of Components
$\square_{A}$	Component A
$\square_{B}$	Component B
$\square_{E}$	Entrainer Component E
$\square_{P}$	Property at Temperature P
$\square_{T}$	Property at Temperature T
$\square_{\mathrm{ex}}$	Experimental Value
$\square^{\mathrm{id}}$	Property for Ideal Mixing Behaviour
$\square^{\mathrm{pure}}$	Pure Component Property
$\square^{\mathrm{E}}$	Excess Property
$\square^{\mathrm{L}}$	Liquid Phase
$\square_{\mathrm{Rel}}$	Relative Value
$\square^{\mathrm{V}}$	Vapor Phase
$\square^{\alpha}$	Phase Indicator
$\square^{\beta}$	Phase Indicator

Abbreviations

NRTL	Non Random Two Liquid
PRO	1-Propanol
WAT	Water
TEG	Triethylene glycol

List of Figures

2.1 As an example for ternary diagrams with isovolatility lines (dashed) and residue curves (dotted), the ternary systems of ethanol - water - ethylene glycol and ethanol - water - glycerol are depicted [5] 4

3.1 Scheme of the VLE602 apparatus used in the laboratory [17] 14
3.2 Calibration lines for the Anton Paar DMA 45 density measurement apparatuses . 16

4.1 Part of the ternary dataset in the format required in the Mathematica regression script 19
4.2 Recorded temperature inside the equilibrium cell 20
4.3 Recorded pressure inside the equilibrium cell 20
4.4 Activity coefficients at infinite dilution, data taken from literature [6], [7] 21
4.5 Excess enthalpy data generated using the UNIFAC model in ASPEN Plus 21

5.1 T-x data of the triethylene glycol - 1-propanol mixture at $P = 100$ [mbar] 26
5.2 T-x data of the triethylene glycol - water mixture at $P = 100$ [mbar] 27
5.3 T-x data of the triethylene glycol - water mixture at $P = 850$ [mbar], from laboratory measurements and literature (see Mostafazadeh, Rahimpour, and Shariati [21]) 28
5.4 T-xy data of the 1-propanol - water mixture at $P = 1$ [atm] from experiments and literature [22], [23], [24] 28
5.5 T-x data of the triethylene glycol - 1-propanol mixture at $P = 100$ [mbar] and boiling curve calculated using the determined NRTL parameters 30
5.6 T-x data of the triethylene glycol - water mixture at $P = 100$ [mbar] and boiling curve calculated using the determined NRTL parameters 30
5.7 T-x data of the triethylene glycol - water mixture at $P = 850$ [mbar] from experiments and literature (see Mostafazadeh, Rahimpour, and Shariati [21]) and boiling curve calculated using the determined NRTL parameters 31
5.8 Infinite dilution activity coefficients γ^{∞} data from literature (Gmehling [6]), together with the NRTL model calculated γ^{∞} over temperature $\frac{1000}{T}$ curve 32
5.9 Infinite dilution activity coefficients γ^{∞} data from literature (Gmehling [7]), together with the NRTL model calculated γ^{∞} over temperature $\frac{1000}{T}$ curve 32
5.10 Activity coefficient curves generated with NRTL parameters of the TEG-PRO system 33
5.11 Activity coefficient curves generated with NRTL parameters of the TEG-WAT system 33

5.12 Relative deviation of the temperature data measured for the ternary system TEG-PRO-WAT 34
5.13 Isovolatility lines in the ternary diagram of the system TEG-PRO-WAT, on molar fraction basis 36
5.14 Pseudo binary McCabe-Thiele diagram of 1-propanol - water mixtures with constant triethylene glycol molar fractions 37
5.15 Residue curves in the ternary diagram of the system TEG-PRO-WAT, on molar fraction basis, as well as univolatility line 38

List of Tables

2.1 Different entrainer properties to be considered during entrainer selection 2

3.1 Entrainer candidates offered for first consideration by the Entrainer Selection software package, based on literature values for infinite dilution activity coefficients, selectivity calculated by software, solvent power calculated from literature and software values 12
3.2 Substances used in the laboratory 13
3.3 Results of gas chromatography measurements on the prepared standard solutions of 1-Propanol and Triethylene glycol 17

4.1 Initial value fields and boundaries for the NRTL parameters used to speed up the regression 24

5.1 Binary interaction parameters determined in the regression 29
5.2 Binary interaction parameters and non-randomness parameters used for further evaluations 34

8.1 Ternary VLE data generated in laboratory experiments using the VLE602 equilibrium still 44
8.2 Material properties used during calculations 45

1 Introduction

Due to the finite nature of products generated from fossil resources, regardless of their purpose or use, opportunities to produce bulk chemicals and energy sources from renewable raw materials remain of interest for a sustainable industrial model. Due to its properties as a solvent and its capability to be used as bio fuel component [1], 1-propanol can be an important component to consider. 1-propanol can be produced from the renewable feedstock glycerol by selective catalytic hydrogenation [2], [3], where finally a mixture of 1-propanol and water is obtained as product. Therefore, a common challenge in 1-propanol purification is the azeotrope it forms with water [4]. To overcome azeotropic behaviour, an extractive distillation process shall be investigated. In extractive distillation commonly a high boiling chemical agent called entrainer is introduced into a distillation process, with the aim of eliminating the azeotropic behaviour through its specific interactions with the present components. [5]

In the present thesis, the steps involved in selecting an entrainer from thermodynamic criteria are outlined. Starting from a group of recommended entrainer candidates, a first assessment of their suitability on the basis of estimated entrainer selectivity is made, and with triethylene glycol a suitable candidate for further investigation is found. To allow more extensive evaluation of the capability of triethylene glycol as entrainer, a vapor-liquid equilibrium data set is compiled from laboratory experiments. This data set comprises measurements of isobaric vapor equilibrium data for all binary subsystems of the ternary mixture present in the proposed extractive distillation process. To analyse the composition of the liquid phase in the laboratory, gas chromatography, Karl-Fischer titration and density measurements are used.

The vapor-liquid equilibrium data are then used, together with infinite dilution activity coefficient data from literature [6], [7], for the determination of model parameters to describe the system. For the thermodynamic description of the system the non random two liquid (NRTL) activity coefficient model is used. The system behaviour described by this NRTL model parameter set is compared to experimentally determined ternary vapor-liquid equilibrium reference data, to ensure adequate description of the ternary behaviour of the mixture by the binary interaction parameters.

Finally, the generated NRTL parameters are used to judge the performance of triethylene glycol by investigating the dependency of the relative volatility of the azeotropic mixture on the amount of triethylene glycol present in the system, as well the minimum entrainer amount necessary to eliminate the azeotropic behaviour. The results generated from this are compared to other entrainers already investigated in literature.

2 Theoretical Background

In the following chapter the theoretical background of the present thesis will be explained concisely. The criteria for the principle task of finding a suitable entrainer for the extractive distillation of the 1-propanol - water mixture are discussed. Expanding from these criteria, the model equations and data needed for a comprehensive understanding of the behaviour of the mixture are explained, which are necessary to reach a verdict on the feasibility of triethylene glycol as an entrainer. If not stated otherwise, the information in this chapter is taken from Gmehling et al. [8].

2.1 Extractive Distillation

Extractive distillation is a unit operation commonly used to separate strongly non-ideal mixtures as for example azeotropic mixtures. The principle relies on the entrainer showing stronger interaction with one of the components of a binary mixture to be distilled, thus enabling the separation into ideally a pure fraction of one component and a new mixed fraction of the entrainer and the second component. Multiple properties are to be considered when choosing a suitable entrainer. Various properties of different value and influence are listed below (table 2.1). [5]

While the general properties listed are certainly important criteria for an entrainer in a cost effective and sustainable process, they themselves do not guarantee a working unit operation; therefore they can be secondary to thermodynamic criteria.

Table 2.1: Different entrainer properties to be considered during entrainer selection

General properties	Availability Cost in procurement Toxicity Flammability Corrosivity
Thermodynamic properties	High selectivity toward one component High (or low) relative volatility Low molar volume and specific heat capacity Low enthalpy of evaporation Does not form new azeotropes with present components
Process specific properties	Necessary entrainer-feed flow ratio Necessary reflux ratio Necessary reboil ratio

The low specific heat capacity and low enthalpy of evaporation are properties important to consider, since they directly influence reboiler and condenser duties. Also the criteria of high relative volatility and the avoidance of forming new azeotropes are important. Depending on whether a high or low boiling entrainer will be used, the relative volatility should depart noticeably from that of the component interacting with the entrainer. Only then an effective solvent recovery is possible. While high boiling entrainers show a higher popularity, the usage of low boiling entrainers is feasible when the process is adapted accordingly. The process specific properties as listed above (table 2.1), while important to consider for the feasibility of the process, require in depth knowledge of the properties of the entrainer and its mixture with the components. The decisive factor in the first entrainer survey is therefore the criterion of high selectivity toward one component. The selectivity is an adaption of the relative volatility α in presence of an entrainer, as presented in equation (2.1). It is the relation of the activity coefficients at infinite dilution γ^{∞} of species A and B, each diluted in species E, the entrainer. Other than the relative volatility α, the selectivity neglects the ratio of the vapor pressures. [5]

$$S^{\infty}_{A,B} = \frac{\gamma^{\infty}_{A}}{\gamma^{\infty}_{B}} \tag{2.1}$$

To allow for separation in the distillation column, the selectivity should depart as far as possible from 1. To allow for better comparison of multiple entrainers, the entrainer capacity $C^{\infty}_{B,E}$ can be introduced, as seen below in equation (2.2). [5]

$$C^{\infty}_{B,E} = \frac{1}{\gamma^{\infty}_{B}} \tag{2.2}$$

The product of the selectivity $S^{\infty}_{A,B}$ and the capacity $C^{\infty}_{B,E}$ is then called the 'solvent power' and is used to compare the entrainers. Only entrainers of the same group (low or high boiling entrainers) should be compared by this method. To supplement this data, ternary diagrams with isovolatility curves ($\alpha_{A,B} = \text{const.}$), as pictured in figure 2.1, should be generated. These require more extensive knowledge of the behaviour of the systems, i.e. a set of viable model parameters. [5]

These diagrams offer insight into the course of residue lines and isovolatility lines, whose dependency on the entrainer concentration is of interest, as the effort of the separation directly depends on these parameters. The intersection of the univolatility line ($\alpha_{A,B} = 1$) and the line of $x_B = 0$ also gives the minimum entrainer amount, which is the necessary mole fraction of entrainer E to eliminate the azeotrope of components A and B. [5]

$$\alpha_{A,B} = \frac{\gamma_A P^{\mathrm{S}}_{A}}{\gamma_B P^{\mathrm{S}}_{B}} \tag{2.3}$$

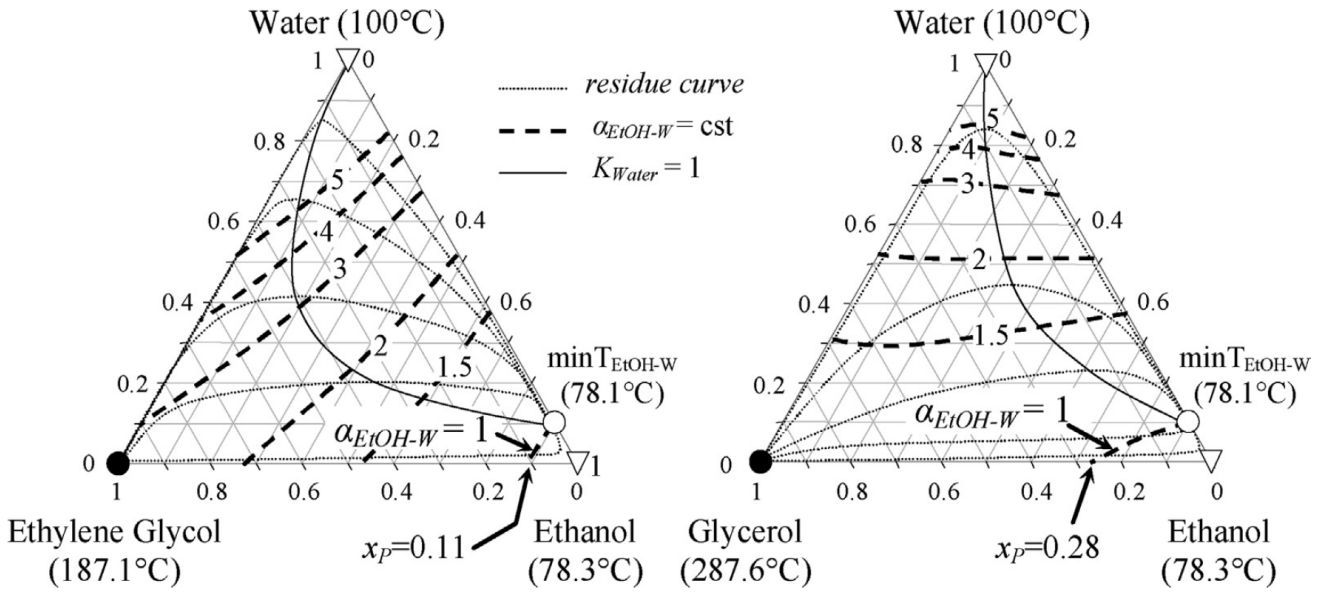

Figure 2.1: As an example for ternary diagrams with isovolatility lines (dashed) and residue curves (dotted), the ternary systems of ethanol - water - ethylene glycol and ethanol - water - glycerol are depicted [5]

The relative volatility $\alpha_{A,B}$ is calculated as seen in equation (2.3) and can be used to quantify the influence of the entrainer on the azeotropic system. The bigger the departure of the relative volatility from unity in proximity to the pure entrainer region, the higher the influence of the entrainer on the system and potentially also the easier the separation of the system. [5]

2.2 Phase Equilibrium

The state of a system containing multiple components is dependent on its temperature, pressure and composition. The initial step for the description of the state of such a system is its equilibrium condition. A defining condition for thermodynamic equilibrium between two phases α and β, besides equal temperature and pressure, is the equal chemical potential μ_i. [6], [8]

$$\mu_i^{\alpha} = \mu_i^{\beta} \tag{2.4}$$

The chemical potential has been proven, applying the Gibbs-Duhem equation, to be identical to the partial molar Gibbs energy $\overline{g_i}$. [8]

$$\overline{g_i}^{\alpha} = \overline{g_i}^{\beta} \tag{2.5}$$

Partial molar properties like these are used to describe the effect of mixing pure components, on the properties of the resulting mixture. If the mixing had no effect at all, the properties could be simply determined by averaging the pure component properties weighted by their mole fractions.

$$g = \sum_i z_i g_i \tag{2.6}$$

Since this is not usually the case, the partial molar properties are introduced to describe the mixing effect. Originating from the total differential of an extensive state variable, partial molar properties regard the effect of the changing fraction of i at constant temperature and pressure. The mole numbers of all components other than i are also constant.

$$\overline{g_i} \equiv \left(\frac{\partial (n_T g)}{\partial n_i} \right)_{T,P,n_{j \neq i}} \tag{2.7}$$

By their definition, and provable by application of the Euler Theorem, the partial molar properties replace the pure component properties in equation 2.6 to describe the mixing effect. [8]

$$g = \sum_i z_i \overline{g_i} \tag{2.8}$$

2.2.1 Vapor Liquid Equilibrium

The partial molar Gibbs energy is expressible as a function of the fugacity. This auxiliary property was established by Lewis to allow the description of the Gibbs energy residual in real fluids similar to ideal gases and can analogously be used to describe the partial molar Gibbs energy in real fluids.

$$\overline{g_i}\left(T, P, z_i\right) = g_i^{\text{pure}}\left(T, P^0\right) + \mathrm{R}T \ln \frac{f_i\left(T, P, z_i\right)}{f_i^0\left(T, P^0\right)} \tag{2.9}$$

Since, as stated above, temperature and pressure in a system in equilibrium must be equal in all phases, their dependent properties g_i^{pure} and f_i^0 must also be equal. Therefore, when inserting into equation (2.5) the definition for the partial molar Gibbs enthalpy of equation (2.9) for two phases α and β, only the fugacities of the phases remain. The equal fugacities f_i across all phases as written in equation (2.10) present a new equilibrium condition.

$$f_i^\alpha = f_i^\beta \tag{2.10}$$

This is called the isofugacity condition. Since the fugacity is a calculatory auxiliary quantity its translation into measurable physical properties is important. For vapor-liquid equilibria, this translation follows two approaches, approach A and B. In both approaches the fugacities are

expressed through coefficients, tying in the physical properties of the system, namely the fugacity coefficients φ_i as defined in equation (2.11) and the activity coefficient γ_i in equation (2.12).

$$\varphi_i^\alpha \equiv \frac{f_i^\alpha}{z_i^\alpha P} \tag{2.11}$$

$$\gamma_i \equiv \frac{f_i^{\mathrm{L}}}{x_i f_i^{0,\mathrm{L}}} \tag{2.12}$$

Approach A, as seen in equation (2.13), uses vapor and liquid phase fugacity coefficients which are usually determined from an equation of state.

$$x_i \varphi_i^{\mathrm{L}} P = y_i \varphi_i^{\mathrm{V}} P \tag{2.13}$$

Approach B, as seen in equation (2.14), uses a vapor phase fugacity coefficient and an activity coefficient to describe the liquid phase behaviour.

$$x_i \gamma_i {f_i^0}_{T,P} = y_i \varphi_i^{\mathrm{V}} P \tag{2.14}$$

For approach B the standard fugacity f_i^0 must then be determined. This can be done by expressing the standard fugacity through the boiling pure liquid at system temperature. Then, only correction for the pressure is necessary.

$${f_i^0}_{T,P} = {f_i^0}_{T,P^0} \exp\left(\frac{v_i^L \left(P - P_i^0\right)}{\mathrm{R}T}\right) = \varphi_i^{\mathrm{S}} P_i^{\mathrm{S}} \exp\left(\frac{v_i^L \left(P - P_i^{\mathrm{S}}\right)}{\mathrm{R}T}\right) = \varphi_i^{\mathrm{S}} P_i^{\mathrm{S}} \mathrm{Poy}_i \tag{2.15}$$

The term Poy_i, used for this pressure correction, stems from the integration of the pressure dependency of the fugacity and is called Poynting factor. For pressure differences below a certain magnitude this correction factor is approximately $\mathrm{Poy}_i = 1$. Also, when dealing with non associating components, the difference of the vapor phase fugacity coefficient φ_i^{L} and the fugacity coefficient of the pure component at saturation φ_i^{S} is negligible, therefore leading to a simplified relation of the phases as seen in equation (2.16).[8]

$$x_i \gamma_i P_i^{\mathrm{S}} \approx y_i P \tag{2.16}$$

When applying the boiling condition, the resulting equilibrium relation is further simplified and suitable for usage in regression of (T, P, x) vapor-liquid equilibrium data sets.

$$P = \sum_i x_i \gamma_i P_i^{\mathrm{S}} \tag{2.17}$$

2.2.2 Mixing Enthalpy

The partial molar Gibbs energy can be further divided into the partial molar Gibbs energy for an ideal mixing effect and a partial molar excess Gibbs energy.

$$\overline{g_i} = \overline{g_i}^{\mathrm{id}} + \overline{g_i}^{\mathrm{E}} \tag{2.18}$$

As described in chapter 2.2.1, the partial molar Gibbs enthalpy can be expressed as a function of fugacity. Equation (2.9) can also be written as equation (2.19).

$$\overline{g_i} = g_i^{\mathrm{pure}}(T, P^0) + \mathrm{R}T \ln x_i + \mathrm{R}T \ln \frac{f_i}{x_i f_i^0} \tag{2.19}$$

This expression (equation(2.19)) follows the same structure as equation (2.18). In fluids conforming to ideal mixing the last term in equation (2.19) equals zero, as the partial molar excess Gibbs energy $\overline{g_i}^{\mathrm{E}}$ does by its definition. Therefore it can be stated, that these two terms equal each other (equation (2.20)).

$$\overline{g_i}^{\mathrm{E}} = \mathrm{R}T \ln \frac{f_i}{x_i f_i^0} = \mathrm{R}T \ln \gamma_i \tag{2.20}$$

The thermodynamic definition for the Gibbs energy also holds true for partial molar excess properties (see equation (2.21)).

$$\frac{\overline{g_i}^{\mathrm{E}}}{\mathrm{R}T} = \frac{\overline{h_i}^{\mathrm{E}} - T\overline{s_i}^{\mathrm{E}}}{\mathrm{R}T} \tag{2.21}$$

The temperature differential at constant pressure of equation (2.21) leads to a description of the excess enthalpy by the excess Gibbs energy, analogous to the Gibbs-Helmholtz equation. The first form of the differential still includes the excess entropy of the mixture, as seen in equation (2.22).

$$\left(\frac{\partial\left(\frac{\overline{g_i}^{\mathrm{E}}}{\mathrm{R}T}\right)}{\partial T}\right)_P = \frac{\left(\frac{\partial \overline{h_i}^{\mathrm{E}}}{\partial T}\right)_P - \overline{h_i}^{\mathrm{E}}\mathrm{R}}{(\mathrm{R}T)^2} - \frac{\overline{s_i}^{\mathrm{E}}\mathrm{R}T + \left(\frac{\partial \overline{s_i}^{\mathrm{E}}}{\partial T}\right)_P \mathrm{R}T^2 - \overline{s_i}^{\mathrm{E}}\mathrm{R}T}{(\mathrm{R}T)^2} \tag{2.22}$$

Due to the definition of the enthalpy, the relation given in equation (2.23) can be assumed.

$$\left(\frac{\partial \overline{h_i}^{\mathrm{E}}}{\partial T}\right)_P = T\left(\frac{\partial \overline{s_i}^{\mathrm{E}}}{\partial T}\right)_P \tag{2.23}$$

Therefore, the temperature differential of equation (2.22) can be simplified to express the Gibbs-Helmholtz equation for partial molar excess properties (equation (2.24)).

$$\left(\frac{\partial\left(\frac{\overline{g_i}^{\mathrm{E}}}{\mathrm{R}T}\right)}{\partial T}\right)_P = -\frac{\overline{h_i}^{\mathrm{E}}}{\mathrm{R}T^2} \tag{2.24}$$

Using equation (2.20) the partial molar excess enthalpy can therefore be written as a function of the activity coefficients γ_i.

$$\frac{\overline{h_i}^{\mathrm{E}}}{\mathrm{R}T^2} = -\left(\frac{\partial\left(\ln\gamma_i\right)}{\partial T}\right)_P \tag{2.25}$$

As stated above in equation (2.8), partial molar properties multiplied with their respective mole fractions allow direct summation to calculate mixture properties. This also applies to the excess enthalpy h^{E}.

$$h^{\mathrm{E}} = \sum_i x_i \overline{h_i}^{\mathrm{E}} \tag{2.26}$$

When combining equation (2.25) and equation (2.26) a relation remains, that can be used for parameter regression. [8]

$$h^{\mathrm{E}} = -\mathrm{R}T^2 \sum_i x_i \left(\frac{\partial \ln\gamma_i}{\partial T}\right)_P \tag{2.27}$$

2.3 The Non-Random-Two-Liquid Model

The Non-Random-Two-Liquid (NRTL) model is a local composition model for the expression of excess properties, specifically the excess Gibbs energy. It expresses the excess Gibbs energy as a function of local compositions and parameters to account for non random behaviour.

When looking at a subsystem of a binary mixture of two substances 1 and 2 with a molecule of species 1 at its center and molecules of substance 1 and 2 in its surroundings, the residual Gibbs energy corresponds to the sum of molecule specific residual Gibbs energies of substance 1, interacting either with a molecule of the same substance 1, or the other substance 2, weighted by the local mole fractions of these interactions x_{11} and x_{21} (equation (2.28)).

$$g_{(1)} = x_{11}g_{11} + x_{21}g_{21} \tag{2.28}$$

In the NRTL model, the relation of the local mole fractions x_{ji} is defined as a function of the residual Gibbs energies, as well as the mole fractions and the non randomness factor α_{12}. For the non randomness factor, the condition $\alpha_{12} = \alpha_{21}$ is implicit.

$$\frac{x_{21}}{x_{11}} = \frac{x_2 \exp\left(-\alpha_{12}\frac{g_{21}}{\mathrm{R}T}\right)}{x_1 \exp\left(-\alpha_{12}\frac{g_{11}}{\mathrm{R}T}\right)} \tag{2.29}$$

The local mole fractions are interconnected by equation (2.30).

$$x_{11} + x_{21} = 1 \tag{2.30}$$

By inserting equation (2.30) into the relation of the local mole fractions equation (2.29), the local mole fraction can be expressed using just the mole fractions (x_1, x_2) and the difference of the residual Gibbs energies multiplied by the non randomness factor α_{12}.

$$x_{21} = \frac{x_2 \exp\left(-\alpha_{12}\frac{g_{21}-g_{11}}{\mathrm{R}T}\right)}{x_1 - x_2 \exp\left(-\alpha_{12}\frac{g_{21}-g_{11}}{\mathrm{R}T}\right)} \tag{2.31}$$

For a pure liquid of species 1, equation (2.28) must hold true, leading to the following expression (equation(2.32)).

$$g_{(1)}^{\mathrm{pure}} = x_{11} g_{11} \tag{2.32}$$

The above equations ((2.28),(2.29),(2.30),(2.31),(2.32)) also apply to a subsystem with a molecule of substance 2 at its center, if all the indices are swapped.

The excess Gibbs energy g^{E} can be determined as the sum of the differences of residual Gibbs energies in pure substance and mixture subsystems, again, weighted by the mole fractions describing the occurrence of the subsystems (equation (2.33)).

$$g^{\mathrm{E}} = x_1 \left(g_{(1)} - g_{(1)}^{\mathrm{pure}}\right) + x_2 \left(g_{(2)} - g_{(2)}^{\mathrm{pure}}\right) \tag{2.33}$$

When inserting equation (2.28), (2.31) and (2.32) into equation (2.33), the NRTL equation is reached (equation (2.34)).

$$g^{\mathrm{E}} = \frac{x_1 x_2 \exp\left(-\alpha_{12}\frac{g_{21}-g_{11}}{\mathrm{R}T}\right)}{x_1 - x_2 \exp\left(-\alpha_{12}\frac{g_{21}-g_{11}}{\mathrm{R}T}\right)}(g_{21} - g_{11}) + \frac{x_2 x_1 \exp\left(-\alpha_{12}\frac{g_{12}-g_{22}}{\mathrm{R}T}\right)}{x_2 - x_1 \exp\left(-\alpha_{12}\frac{g_{12}-g_{22}}{\mathrm{R}T}\right)}(g_{12} - g_{22}) \tag{2.34}$$

To shorten the notation of NRTL equations the parameters τ and G are introduced. The parameter τ represents the difference of Gibbs energies. The equation below describes τ_{21}, the parameter τ_{12} can be reached simply by swapping the indices 1 and 2.

$$\tau_{21} = \frac{g_{21} - g_{11}}{\mathrm{R}T} \tag{2.35}$$

The parameter G represents the exponential function of τ multiplied with the negative non randomness factor $-\alpha_{12}$. Again, the equation (2.36) below states G_{21}, G_{12} can be reached by swapping the indices 1 and 2 (the condition for the non randomness factor $\alpha_{12} = \alpha_{21}$ still applies).

$$G_{21} = \exp\left(-\alpha_{12}\tau_{21}\right) \tag{2.36}$$

The NRTL equation is usually given using these parameters τ and G as seen below in equation

(2.37).

$$\frac{g^{\mathrm{E}}}{\mathrm{R}T} = \frac{x_1 x_2 G_{21}}{x_1 - x_2 G_{21}}\tau_{21} + \frac{x_2 x_1 G_{12}}{x_2 - x_1 G_{12}}\tau_{12} \tag{2.37}$$

The activity coefficients of the substances can then be determined from equation (2.37) through differentiation. [9]

$$\ln \gamma_1 = {x_2}^2 \left(\tau_{21} \frac{{G_{21}}^2}{\left(x_1 + x_2 G_{21}\right)^2} + \tau_{12} \frac{G_{12}}{\left(x_2 + x_1 G_{12}\right)^2} \right) \tag{2.38}$$

2.3.1 Fitting NRTL Model Parameters

The process of finding new viable parameters for the NRTL g^{E} model requires the description of the behaviour of experimentally determined data through the parameter τ as introduced in equation (2.35). This parameter, originally introduced to represent the interaction of molecules, is therefore described by a temperature dependent polynomial, whose parameters can be fitted to the experimental data.

$$\tau_{ij} = A_{ij} + \frac{B_{ij}}{\theta} + E_{ij} \ln \theta + F_{ij}\theta \tag{2.39}$$

In equation (2.39) the variable θ represents a dimensionless temperature value as reached by equation (2.40).

$$\theta = \frac{T\ [\mathrm{K}]}{1\ [\mathrm{K}]} \tag{2.40}$$

Depending on the expected or observed dependency of the system on the temperature, the polynomial (equation (2.39)) may be reduced to versions using only the A_{ij} and B_{ij} terms. [8]

2.3.2 Activity Coefficients at Infinite Dilution

As stated above in chapter 2.1, the activity coefficients at infinite dilution γ_i^{∞} are commonly used to evaluate the suitability of entrainers for extractive distillation. Their accurate description is also an important factor in the description of distillation processes, due to their influence on the number of theoretical separation stages. [8]

The equation for the activity coefficients in a binary mixture (equation 2.38) shows the dependency of the activity coefficient γ_i on the molar fraction x_i. When applying the condition of infinite dilution as stated in equation (2.41), equation (2.38) can be simplified.

$$\ln \gamma_i|_{x_i \to 0} = \ln \gamma_{ij}^{\infty} \tag{2.41}$$

In a binary mixture, the reduction of one molar fraction $x_1 \to 0$ requires the increase of the

other molar fraction towards $x_2 \to 1$. The resulting equation (2.42) for the activity coefficients at infinite dilution is given below.[8], [10]

$$\ln \gamma_{ij}^{\infty} = \tau_{ji} - \tau_{ij} G_{ij} \tag{2.42}$$

3 Materials and Methods

3.1 Determination of Suitable Entrainers

As explained in chapter 2.1, the suitability of an entrainer relies on multiple aspects all based on profound knowledge of the behaviour of the different components and their mixtures. The values of selectivity and solvent power as introduced in the aforementioned chapter were taken as first indicators in the search for relevant entrainers.

To quickly generate a first list of candidates, Entrainer Selection, a Dortmund Data Bank software package, was used. This program assembles a first summary of possible entrainers for a given azeotropic mixture, will however rely on estimation methods if the behaviour of a possible candidate is insufficiently documented in the databases. The first list of candidates formulated after usage of Entrainer Selection is given below in table 3.1.

Table 3.1: Entrainer candidates offered for first consideration by the Entrainer Selection software package, based on literature values for infinite dilution activity coefficients, selectivity calculated by software, solvent power calculated from literature and software values

Entrainer Candidate	Selectivity S_{12}^{∞} [-]	Solvent Power $S_{AB}^{\infty} * C_{BE}^{\infty}$ [-]
Glycerol	7.47	8.06
Diethylene glycol	2.20	2.76
Ethylene glycol	2.06	1.70
Triethylene glycol	1.90	2.73
Sulfolane	1.62	0.66
Dimethyl sulfoxide	1.55	4.07
1,4-Butanediol	1.45	1.38
N,N-Dimethylformamide	0.60	-
N-Methyl-2-pyrrolidone	0.60	-

The two last listed candidates, N,N-Dimethylformamide and N-Methyl-2-pyrrolidone, are excluded from further consideration since their selectivity values below $S_{12}^{\infty} = 1$ necessitate a different process flow scheme and therefore their behaviour, although potentially suitable for extractive distillation, is not directly comparable to the rest of the candidates. Also their selectivity may roughly be compared to the rest by computing the inverse, which remains lower than those of the more promising candidates on top of the list. The solvent power as stated in 3.1 is calculated from literature data and the results of Entrainer Selection according to equation (3.1) for further filtering of the candidates.

$$S_{AB}^{\infty} * C_{BE}^{\infty} = \frac{\gamma_A^{\infty}}{\gamma_B^{\infty}} * \frac{1}{\gamma_B^{\infty}} \tag{3.1}$$

Its consideration leads to the exclusion of Sulfolane and 1,4-Butanediol because of their low selectivity and solvent power. Dimethyl sulfoxide was ruled out due to concerns regarding its possible auto-catalytic decay [11]. As the data situation of Ethylene glycol and Glycerol in mixtures with 1-propanol and water was found to already be sufficient for later comparisons ([4], [12]), as well as due to the toxicity of Ethylene glycol and Diethylene glycol ([13], [14]) and due to concerns over Glycerol's comparatively high viscosity ([15], [16]) having an effect on the separation, the remaining promising candidate for further investigation was determined to be Triethylene glycol (TEG).

3.2 Laboratory Materials

The main aspects of the laboratory work for this project was the measurement of vapor-liquid equilibria of the 1-propanol - water - triethylene glycol system. The vapor and liquid samples were analysed using gas chromatography, density measurements and Karl-Fischer titration methods. In the table below all used substances are listed, including their respective purity (table 3.2).

Table 3.2: Substances used in the laboratory

Material	Manufacturer	Purity
Water	Roth	≤ 2.0 [μS/cm], double distilled
Ethanol	Roth ROTIPURAN	$\geq 99.8\%$ p.a. denat.
1-Propanol	Roth ROTIPURAN	$\geq 99.5\%$
Triethylene glycol	Sigma Aldrich	$\geq 99\%$

3.3 VLE Apparatus

The still used in the laboratory is a Fischer Labodest VLE 602 dynamic vapor-liquid equilibrium apparatus. The apparatus is comprised of a mixing and a boiling chamber, an equilibrium cell and separate coolers for the vaporous and liquid phases. The cooled down phases are fed back into the mixing chamber, thus enabling the recycle method of equilibrium determination. In figure 3.1 the diagram of the still is depicted.

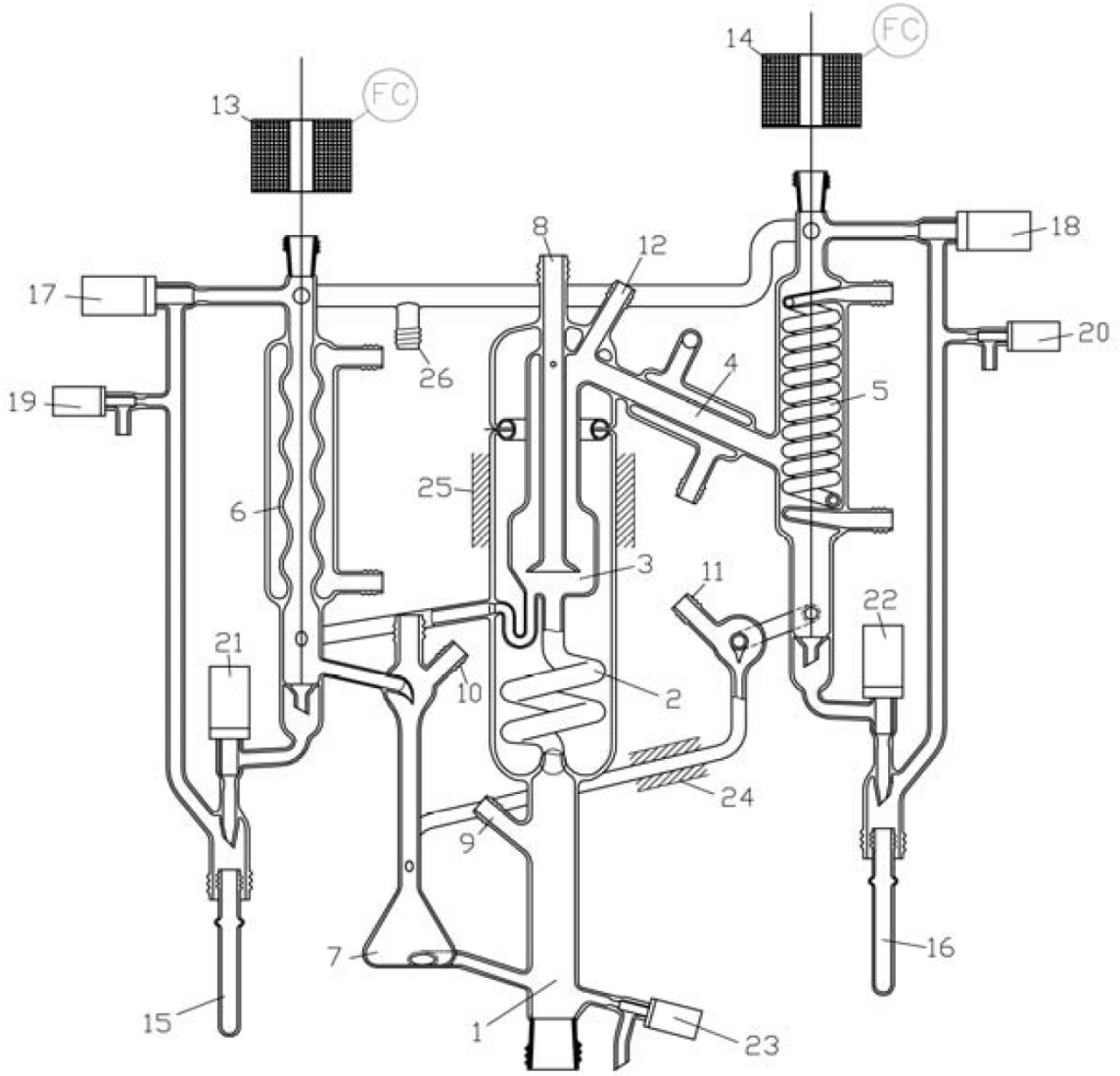

Figure 3.1: Scheme of the VLE602 apparatus used in the laboratory [17]

1	Heater
2	Cottrell Pump
3	Phase separation chamber
4	Condenser
5	Safety condenser: vapor phase
6	Safety condenser: liquid phase
7	Mixing chamber w. stirrer
8	Pt100: equilibrium cell temperature
9	Pt100: heating cell temperature
10	Septum: sample liquid phase
11	Septum: sample condensed vapor phase
12	Septum: sample vapor phase
13	Magnetic coil: sample liquid phase
14	Magnetic coil: sample vapor phase
15	Sample vessel: liquid phase
16	Sample vessel: vapor phase
17	Pressure valve: liquid phase sample
18	Pressure valve: vapor phase sample
19	Pressure release valve: liquid phase
20	Pressure release valve: vapor phase
21	Valve: liquid phase sample
22	Valve: vapor phase sample
23	Mixture release valve
24	Pt100: temperature at capillary
25	Pt100: heating jacket
26	Connection to buffer vessel

The substances are injected into the mixing chamber one after the other, starting with the low boiling component. After the designated substances have been added to the still, the substances are mixed by a magnetic stirrer at the bottom of the mixing chamber. Utilising sufficient mixing power, the substances used should become a homogeneous mixture, at least at the entrance to the boiling chamber. In the boiling chamber a quartz heater heats the mixture until partial vaporisation takes place. Steady formation of bubbles along the surface of the heater can be observed. The Cottrell-pump above the heater is formed, so that it maximises the mass transport between the vapor and liquid phases, the liquid phase being pulled up and through the pump by the rapidly rising bubbles. The phase separation chamber is situated above the top outlet of the Cottrell-pump and formed to separate the vapor phase from the liquid phase. Both phases are then fed into their coolers. The vapor phase passes a counter current Liebig condenser, functioning as main condensator. The emerging stream is further cooled by a spiral condenser to ensure complete condensation of the phase and prohibit any components form exiting the apparatus through the gas outlet. The liquid phase stream is also led through the bottom of an Allihn condenser to prevent any evaporating fractions in the liquid stream from leaving the apparatus. The fully condensed phases are fed back into the mixing chamber.

During operation, the system is closed to allow different operating pressures. The pressures of the measurements range from 100 [mbar] to 1100 [mbar], the apparatus allows up to 4000 [mbar]. To still allow samples to be taken during live operation, the apparatus is equipped with valves and a pressure equalization system for the sample vessels. This system however needs a certain volume of samples to be accurate, about 5 [ml], therefore a different way of sample taking was employed, using syringes and septa. With this method the sample volume could be kept at about 1 to 2 [ml], if more was not needed. This is of practical importance, as taking out large amounts of substances will inevitably influence the equilibrium state.

The software package included with the system records temperatures and pressure inside the apparatus. The thermometer used for the equilibrium evaluation is inserted from the top into the phase separation chamber to detect the vapor temperature in the equilibrium cell. The thermometer was calibrated using ice water and boiling water as well as a reference thermometer. The pressure sensor was also calculated using a vacuum pump and a reference sensor.

3.4 Analytics

Due to the limitations of the individual analytic methods, samples were analysed in three different ways, depending on their expected components. Binary mixtures were analysed by density measurement if sufficient sample volume was available. If not, and the sample contained water,

Karl Fischer titration was used. If neither criteria applied, gas chromatography was used. Ternary mixtures were always analysed by Karl Fischer titration and gas Chromatography.

3.4.1 Density Measurement

For all density measurements two Anton Paar DMA 45 apparatuses were used. Due to the functionality of these apparatuses, the samples for density measurement need a minimum amount of 2 [ml] to ensure an accurate measurement. Due to the limited sample volume in most experimental runs, density measurements were not suitable for all binary mixture samples. Therefore mainly 1-propanol - water mixtures were analysed by density measurements. The calibration lines determined on the density measurement apparatuses are given below (equation 3.2 & 3.3, diagram 3.2).

$$w_{\mathrm{PRO,AP1}} = -25.654\rho^3 + 65.564\rho^2 - 60.511\rho + 20.585 \tag{3.2}$$

$$w_{\mathrm{PRO,AP2}} = -22.703\rho^3 + 57.848\rho^2 - 53.825\rho + 18.662 \tag{3.3}$$

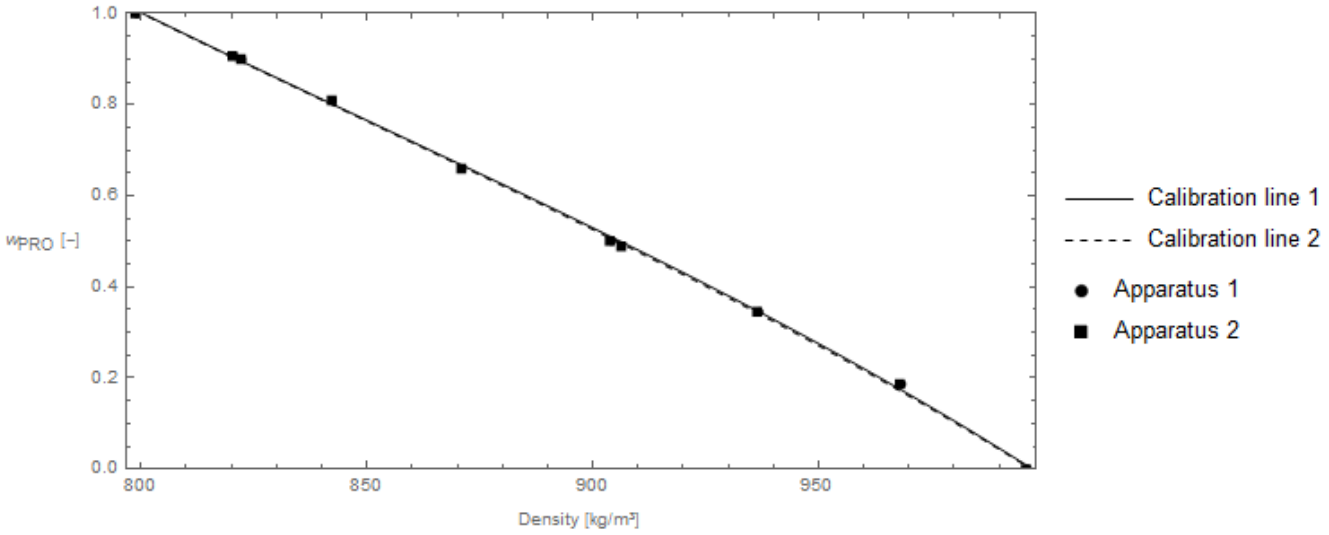

Figure 3.2: Calibration lines for the Anton Paar DMA 45 density measurement apparatuses

3.4.2 Karl Fischer Titration

The samples designated for Karl Fischer titration were diluted using ethanol to ensure a maximum water content of 10%$_{\mathrm{w}}$. Due to the ethanol used for dilution also containing trace amounts of water, its content was determined and taken into account when determining the water content of the original sample. For most samples the dilution ratio was 1:5 or 1:10. The apparatus used

automatically determines the measured samples water content from the injected sample weight as a weight fraction. This value is used to calculate the water weight fractions of the original samples.

$$w_{\text{WAT, sample}} = w_{\text{WAT, measured}} \frac{m_{\text{sample}} + m_{\text{EtOH}}}{m_{\text{sample}}} \tag{3.4}$$

3.4.3 Gas Chromatography

For all measurements in this work a gas chromatograph of the type Agilent 7890 with an automatic sampler and flame ionisation detector was used. All samples were diluted with ethanol to allow for substance measurements in adequately low concentrated regions of up to 15000 [ppm]. In this mass fraction region linear behaviour for the relation of mass fraction and observed conductivity at the detector is assumed. A split injection GC method was used, with a split ratio of 10:1 and a DB624UI column. The gases used were synthetic air and nitrogen as well as hydrogen as a burner gas. The temperature at the inlet was set to 300 [°C], in the oven to 250 [°C] and at the FID to 350 [°C].

For the calibration of the gas chromatograph several standard solutions were prepared. Table 3.3 contains the gravimetrically determined mass fractions and the area under the measured conductivity curve of these standards. From these results, calibration lines were fitted assuming that in the absence of a substance no peak for this substance can be detected. The equation is therefore simplified to the following (equation (3.5)). The k values used can be seen in table 3.3.

$$w_{i,\text{measured}} = kA_i \tag{3.5}$$

Table 3.3: Results of gas chromatography measurements on the prepared standard solutions of 1-Propanol and Triethylene glycol

1-Propanol (k = 0,6923485011)							
Mass fraction	[mg/kg]	117	559	1137	5890	11546	17250
Mean Area	[-]	164,6	842,4	1719,8	8817,3	16824,1	24697
Std.Dev.	[-]	1,715	1,728	6,720	4,216	49,292	308,442
Triethylene glycol (k = 1,8154748184)							
Mass fraction	[mg/kg]	502	1022	5295	10382	15510	
Mean Area	[-]	262,5	562,7	2944,2	5703,8	8543,8	
Std.Dev.	[-]	0,403	2,504	1,886	2,531	20,047	

To determine the actual mass fraction of the component in the original sample before dilution the weight of the diluted sample and the amount of solvent is required, as seen in equation (3.6).

$$w_{i,\text{sample}} = w_{i,\text{measured}} \frac{m_{\text{sample}} + m_{\text{EtOH}}}{m_{\text{sample}}} \tag{3.6}$$

4 Data Processing and Calculations

The vapor liquid equilibrium data generated as described in chapter 3, together with activity coefficient data from literature, act as the basis for the mixture parameter regression. That regression is needed to evaluate the suitability of the investigated Triethylene glycol (TEG) as an entrainer in the extractive distillation of the 1-Propanol - Water mixture.

4.1 Laboratory Data Processing

A complete vapor liquid equilibrium data set as used for further calculations contains data for temperature, pressure and composition of the phases. In figure 4.1 an example for a data set is shown as expected by the Mathematica script used for the further calculations. To distinguish the mass fraction of substances, commonly used in the laboratory, from the molar fraction needed in the NRTL model equations, w' and w'' were used to denote the weight fractions in the liquid and vapor phases. The conversion of weight fractions to molar fractions was included in the Mathematica script. The temperature is expected in [K], the pressure in [mbar]. The standard deviations given in the columns on the right are given in the units of their corresponding entities.

Name	T	P	w'_TEG	w'_PRO	w'_WAT	w''_TEG	w''_PRO	w''_WAT	σ(T)	σ(P)	σ(w')	σ(w'')
Tern0.5_1.01	367,04	1011,06	0,435	0,407	0,167	0,0000	0,7744	0,2256	0,2174	1,3163	0,0020	0,0003
Tern0.5_1.02	364,61	1009,98	0,391	0,316	0,244	0,0000	0,7162	0,2838	0,1654	1,9121	0,0020	0,0002
Tern0.5_1.03	364,03	1011,90	0,350	0,302	0,359	0,0000	0,6754	0,3246	0,0726	1,0338	0,0031	0,0011
Tern0.5_2.01	363,76	1010,86	0,312	0,256	0,439	0,0000	0,6651	0,3349	0,0707	1,0445	0,0016	0,0016
Tern0.5_2.02	363,84	1011,47	0,266	0,219	0,514	0,0000	0,6547	0,3453	0,0798	1,6206	0,0015	0,0018
Tern0.5_2.03	364,09	1011,47	0,244	0,170	0,578	0,0000	0,6452	0,3548	0,0000	1,8599	0,0018	0,0007
Tern0.5_2.04	364,66	1011,80	0,246	0,149	0,698	0,0000	0,6285	0,3715	0,0193	1,9890	0,0009	0,0008

Figure 4.1: Part of the ternary dataset in the format required in the Mathematica regression script

4.1.1 Temperature and Pressure Data

During the operation of the laboratory apparatus, the temperature inside the equilibrium chamber was measured and recorded in [°C]. The recorded temperatures of the relevant time frames for each equilibrium state were then evaluated. A constant temperature over at least 5 minutes with active heating was considered indicative of an equilibrium state inside the cell. The recorded temperatures (as pictured in figure 4.2) were used to find the mean temperature and the standard deviation of each equilibrium state's time frame in [K]. Like the temperature, the pressure inside

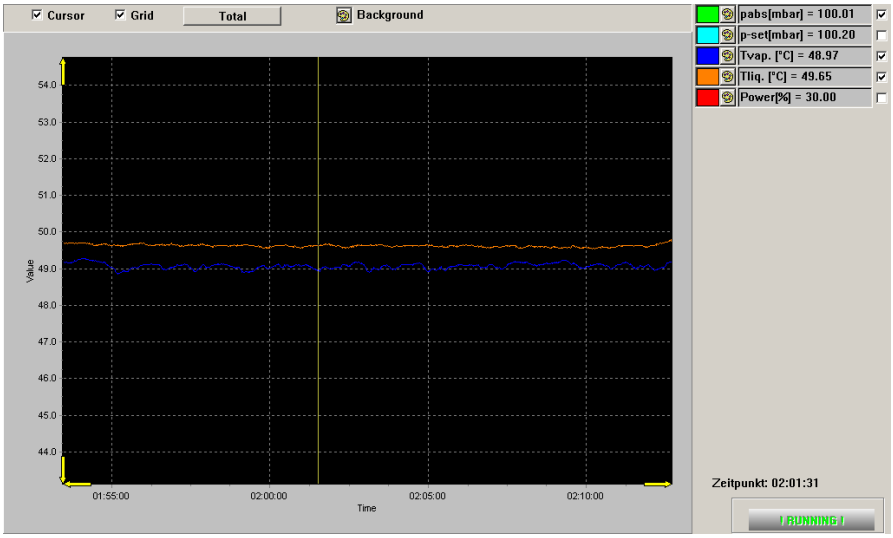

Figure 4.2: Recorded temperature inside the equilibrium cell

the equilibrium cell was recorded during the experiment and constantly regulated. The recorded time frame was matched to that of the temperature and the mean and standard deviation values are determined in [mbar].

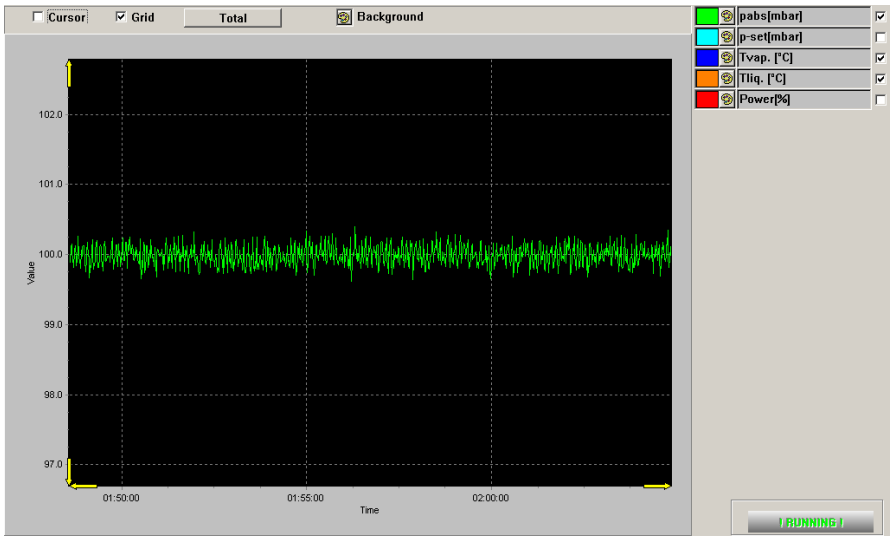

Figure 4.3: Recorded pressure inside the equilibrium cell

4.1.2 Composition Data

As described in chapter 3.4, the weight fractions of the components were calculated from the measurement results. Depending on the measurement, the determination was executed multiple times to account for outliers, usually five measurements of every sample were conducted. The

mean weight fraction of each component and the standard deviation were then determined for each equilibrium state resulting in one data point.

4.2 Literature Data

The data sets for the activity coefficients at infinite dilution γ^{∞} and excess enthalpy h^{E} were taken from literature in the case of γ^{∞} and generated from UNIFAC parameters for testing purposes in the case of h^{E}. The data was then reformatted to allow a consistent automatic import into the Mathematica script. In figure 4.4 an example for the formatted γ^{∞} data is pictured, figure 4.5 shows part of the formatted data for h^{E}, as generated using ASPEN Plus.

Material 1	Material 2	Material index 1	Material index 2	Temperature	Gamma infinite
Water	Triethylene glycol	3	1	323,15	0,67
Water	Triethylene glycol	3	1	328,15	0,672
Water	Triethylene glycol	3	1	333,15	0,685

Figure 4.4: Activity coefficients at infinite dilution, data taken from literature [6], [7]

Source	T [K]	P [mbar]	w'_TEG	w'_PRO	w'_WAT	hE [J/mol]
ASPEN	298,15	1013,25	0,00000	1,00000	0,00000	0,00
ASPEN	298,15	1013,25	0,06667	0,93333	0,00000	30,90
ASPEN	298,15	1013,25	0,13333	0,86667	0,00000	60,22

Figure 4.5: Excess enthalpy data generated using the UNIFAC model in ASPEN Plus

4.3 Material Properties

The properties of all materials relevant to the calculations in the regression were taken from literature and formatted as a table for import into the Mathematica script. Relevant properties are the density ρ, molar mass MM, and the parameters for the Antoine equation A, B, and C, used to calculate the pure component vapor pressure P_i^{s} from the system temperature. In equation (4.1) the used Antoine equation can be seen.

$$\log_{10}\left(P_i^{\mathrm{s}}\ [\mathrm{bar}]\right) = A - \frac{B}{C + T\ [\mathrm{K}]} \tag{4.1}$$

The table of material data can be found in table 8.2, in the appendix. The parameter names A and B mentioned here are specific to the Antoine equation and must not be mistaken for the NRTL parameters A_{ij} and B_{ij}.[18], [19], [20]

4.4 Regression of model parameters

The regression of the parameters for the Non-Random-Two-Liquid activity coefficient model was executed in a Mathematica script. The number of data sets and materials n can be defined to fit varying needs. As mentioned in chapter 2.3, the NRTL model relies on a set of parameters to describe the interaction of the materials by the coefficient τ_{ij}. In this case, a set of three parameters was chosen to describe τ_{ij}, the chosen parameters being, A, B, and F, as illustrated in equations (2.39) and (4.4).

For the regression, the non-randomness parameter $\alpha_{i,j}$ was defined for each pair of substances i and j. All parameters were defined as matrices (list of lists) containing all the values of that specific parameter for each binary system. Equation (4.2) shows α as an example for a system of $n = 3$ materials.

$$\alpha = \begin{pmatrix} \alpha_{11} & \alpha_{12} & \alpha_{13} \\ \alpha_{21} & \alpha_{22} & \alpha_{23} \\ \alpha_{31} & \alpha_{32} & \alpha_{33} \end{pmatrix} = \begin{pmatrix} 0 & 0.30 & 0.30 \\ 0.30 & 0 & 0.47 \\ 0.30 & 0.47 & 0 \end{pmatrix} \tag{4.2}$$

Unlike the matrices of the binary parameters A, B, and F the given α must be symmetric along the main diagonal, as the condition of $\alpha_{ij} = \alpha_{ji}$ must be satisfied. The binary parameters in A_{ij}, B_{ij}, and F_{ij} do not underlie this restriction.

Once the data sets had been imported, the molar fractions of the components were computed as seen in equation (4.3).

$$x_i = \frac{\frac{w_i}{MM_i}}{\sum_i^n \left(\frac{w_i}{MM_i}\right)} \tag{4.3}$$

The model equations were implemented as functions to allow for more flexibility in the number of components evaluated simultaneously. Equations (4.4), (4.5) and (4.6) show the general equations needed for the activity coefficient of a component γ_i, as well as their functional dependencies. The variable x denotes an array comprised of $(x_i, x_j, ..., x_n)$, so that $\sum x = 1$.

$$\tau_{ij}(A, B, F, T) = A_{ij} + \frac{B_{ij}}{T} + F_{ij}T \tag{4.4}$$

$$G_{ij}(A, B, F, T) = \exp\left(-\alpha_{ij}\tau_{ij}\right) \tag{4.5}$$

$$\ln \gamma_i(x, A, B, F, T) = \frac{\sum_j \tau_{ji} G_{ji} x_j}{\sum_k G_{ki} x_k} + \sum_j \frac{G_{ij} x_j}{\sum_k G_{kj} x_k} \left(\tau_{ij} - \frac{\sum_n \tau_{nj} G_{nj} x_n}{\sum_k G_{kj} x_k}\right) \tag{4.6}$$

These functions are evaluated multiple times during regression, which is based on the minimization of an objective function.

4.4.1 Objective Function

The objective function is a function comprising the 'Errors' of the model calculated system properties when compared to the measured properties. For the regression of vapor-liquid equilibria various objective functions can be used. Depending on the type of data available, as well as the purpose of the parameters achieved, a different decision can be made when choosing the objective function to be used. [8]

For this project, an objective function Obj comprising TPx vapor-liquid equilibrium data, γ^{∞} data and optionally also h^{E} data was chosen, the different error terms were taken from literature ([8]). The vapor-liquid equilibrium data was represented by a pressure term. The full objective function can be seen in equation (4.7) below. In this equation the weighting factors, used to control the influence of the data types on the objective function are denoted as ω_{P}, $\omega_{\gamma^{\infty}}$ and $\omega_{h^{\mathrm{E}}}$.

$$Obj = \omega_{\mathrm{P}} \sum \left(\frac{P - P_{\mathrm{ex}}}{P_{\mathrm{ex}}} \right)^2 + \omega_{\gamma^{\infty}} \sum \left(\frac{\gamma_i^{\infty} - \gamma_{i,\mathrm{ex}}^{\infty}}{\gamma_{i,\mathrm{ex}}^{\infty}} \right)^2 + \omega_{h^{\mathrm{E}}} \sum \left(\frac{h^{\mathrm{E}} - h_{\mathrm{ex}}^{\mathrm{E}}}{h_{\mathrm{ex}}^{\mathrm{E}}} \right) \tag{4.7}$$

The pressure in the system was implemented as seen below (equation (4.8)). The composition data x and the temperature data T were taken from the laboratory data during the evaluation of the objective function.

$$P(x, A, B, F, T) = \sum_{i}^{n} x_i \gamma_i P_i^{\mathrm{s}} \tag{4.8}$$

The activity coefficients at infinite dilution were calculated using a function equal to equation (4.9), an implementation of equation (2.42).

$$\gamma^{\infty}(i, j, A, B, F, T) = \exp\left(\tau_{ji} - \tau_{ij} G_{ij}\right) \tag{4.9}$$

Lastly, the excess enthalpy h^{E} was implemented as a function corresponding to equation (2.27). Due to missing data, the h^{E} part of the objective function was not activated during the regression of the parameters presented in chapter 5. The possibility to include them however remains part of the Mathematica script, the weighting factor $\omega_{h^{\mathrm{E}}}$ was just set to 0. The weighting factors of vapor-liquid equilibrium data ω_{P} and infinite dilution activity coefficient data $\omega_{\gamma^{\infty}}$ were kept equal.

The regression was performed, using a numerical minimization routine 'NMinimize', which minimizes the objective function multiple times, starting from a set of random values. The routine 'NMinimize' allows for the definition of an initial field of values for the parameters as well as boundaries that should not be exceeded. According to literature, for a system using three param-

eters, no fixed boundaries exist (see Gmehling et al. [8]). The used boundaries, and initial value fields are given in the table below (table 4.1).

Table 4.1: Initial value fields and boundaries for the NRTL parameters used to speed up the regression

Parameter	Region Center	Initial field	Boundaries
A_{ij}	0.00	± 0.50	± 1000
B_{ij}	0.00	± 100.00	± 1000
F_{ij}	0.00	± 0.10	± 100

The given values were found to be beneficial during testing of the script. Too high values for the parameters in F quickly lead to an overflow problem. The initial value field of A was kept low in reference to the limits for a two parameter system, for which the expected limits of $A = \pm 6$ and $B = \pm 1000$ apply.

4.5 Parameter Validation

During the parameter validation the boiling temperature T and the activity coefficients γ_i as a function of the molar fractions x_i, and the activity coefficients at infinite dilution γ_i^∞ as a function of the temperature were calculated.

The temperature T was determined by solving equation (4.10) with Mathematica's 'FindRoot' function. As a starting value for the function $T = 350[K]$ was used.

$$T(x_i, ..., x_n) = \text{Solve}\left[P_{ex} == \sum_i^n x_i \gamma_i P_i^{\text{s}} \ , \ T\right] \tag{4.10}$$

The activity coefficients γ_i were calculated from equation (4.6) using $T(x)$, the infinite dilution activity coefficients γ_i^∞ were calculated according to equation (2.42) as a function of the temperature in intervals relevant to the data from literature.

When comparing data to model results, the mean relative deviation, and the root mean square relative deviation were used. Equation (4.11) and equation (4.12) show how this quantities were determined.

$$\Delta T_{\text{Rel}} = \frac{1}{n_{\text{data}}} * \sum_i^{n_{\text{data}}} \left| \frac{T_i - T_{\text{ex},i}}{T_{\text{ex},i}} \right| \tag{4.11}$$

$$RMSRD_{\gamma^\infty} = \sqrt{\frac{1}{n_{\text{data}}} * \sum_i^{n_{\text{data}}} \left(\frac{\gamma_i^\infty - \gamma_{\text{ex},i}^\infty}{\gamma_{\text{ex},i}^\infty} \right)^2} \tag{4.12}$$

4.6 Entrainer Evaluation

The relative volatility, as used to compare the entrainers properties, was calculated using equation (2.3). It was determined for the whole molar fraction region of the ternary mixture, to find all lines of univolatility and isovolatility.

The residue curves plotted were calculated using numerical integration of the differential equation for open evaporation, also called Rayleigh equation. The equation is stated below in equation 4.13 using a non-linear dimensionless timescale $\mathrm{d}\xi = \frac{\mathrm{d}L}{L}$. [8]

$$\frac{\mathrm{d}x_i}{\mathrm{d}\xi} = y_i - x_i \tag{4.13}$$

The numerically integrated form (equation(4.14)) was then used for the iterative calculation of the composition points along the residue curve in the ternary diagram.

$$x_{i,k} = x_{i,k-1}\left(1 + \Delta\xi\left(\frac{y_{i,k-1}}{x_{i,k-1}} - 1\right)\right) \tag{4.14}$$

5 Results and Discussion

5.1 Experimental Data

In the laboratory, data sets of binary mixture vapor-liquid equilibria were generated for the regression of the binary interaction parameters, as well as data sets of ternary mixture vapor-liquid equilibria, which were only used for the validation of the computability of ternary mixture behaviour from binary mixture parameters. In the following, only the data points themselves were examined and compared to reference data from literature sources.

The following diagram (figure 5.1) shows the data obtained in the laboratory for a binary mixture of triethylene glycol and 1-propanol (TEG-PRO). The data stem from three consecutive experimental runs, each started with pure 1-propanol and triethylene glycol was added in small doses between each equilibrium point.

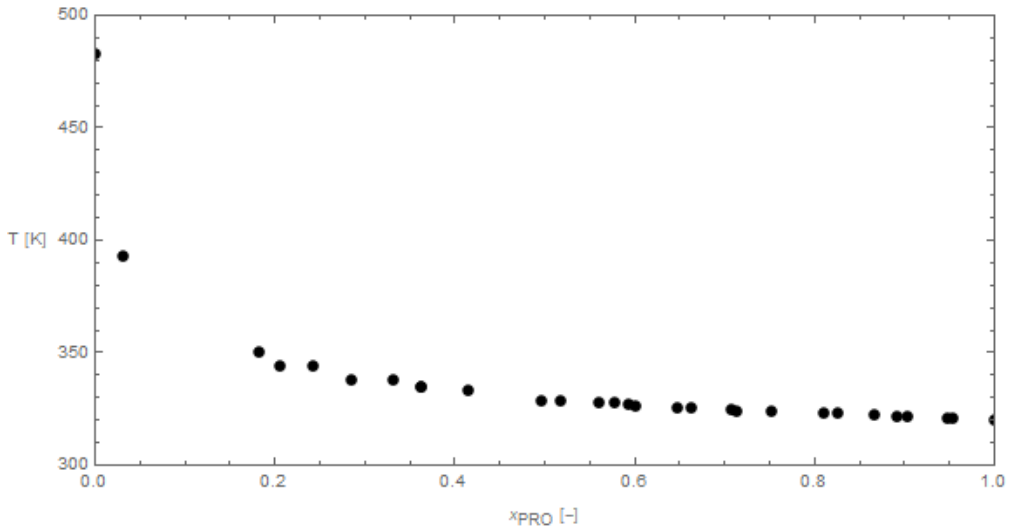

Figure 5.1: T-x data of the triethylene glycol - 1-propanol mixture at $P = 100$ [mbar]

During the experimental runs a tendency of the system was observed, where the system temperature showed oscillating behaviour during operation with small weight fractions of 1-propanol. The determination of a stable equilibrium point was therefore not always possible. Some equilibria where the temperature remained stable for time periods of at least 5 minutes were however achieved. Nevertheless, these difficulties are the reason for the observable gap between the data points around $x_{\mathrm{PRO}} = 0.1$ in figure 5.1 above. The gap is also exacerbated by the conversion

of weight fractions w_i to molar fractions x_i, as it distorts the data set along the abscissa. The definitive reason for the difficulties in achieving equilibrium in this molar fraction region could not be determined. A possible reason may be a periodic oscillation of the liquid phase composition when the flow of distillate back into the mixing chamber is somehow inhibited, as the distillate stream is very small during operation with small weight fractions of 1-propanol in the liquid phase, probably owing to the high vapor phase purity.

In figure 5.2 the data points obtained during experiments with the binary mixture of triethylene glycol and water are depicted. Four experimental runs with this binary system were performed consecutively, each started with pure water and triethylene glycol added in small doses.

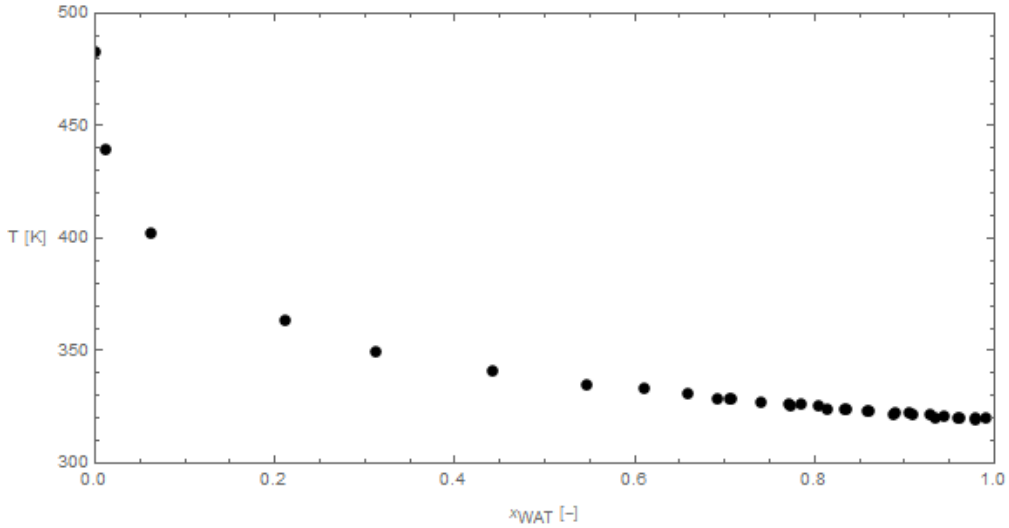

Figure 5.2: T-x data of the triethylene glycol - water mixture at $P = 100$ [mbar]

The diagram also shows the behaviour already described for the binary system TEG-PRO, of the data points seemingly thinning toward the region of low water content. This can again be explained by the conversion of weight fractions w_i, with which the positions of the data points were estimated in the laboratory, to molar fractions x_i, as the molar weight of water is significantly lower than that of triethylene glycol (see [18] and [20]).

All in all, the data points generated for the binary systems TEG-PRO and TEG-WAT show reasonable behaviour, no wrongly determined azeotropes or mixing gaps can be observed.

While the first three experimental runs were performed at $P = 100$ [mbar], the fourth was performed at $P = 850$ [mbar] so that it could be compared to literature data. The comparison can be seen in the diagram below (figure 5.3). While the measurements only cover a smaller range of molar fraction, than the literature data, it can be stated that the data points agree with the literature data, as the overall trends seem to coincide. Since the experimental data were only

generated for validation reasons and not for regression, this agreement shall suffice to say that the data generated with this experimental set up can be regarded as reliable.

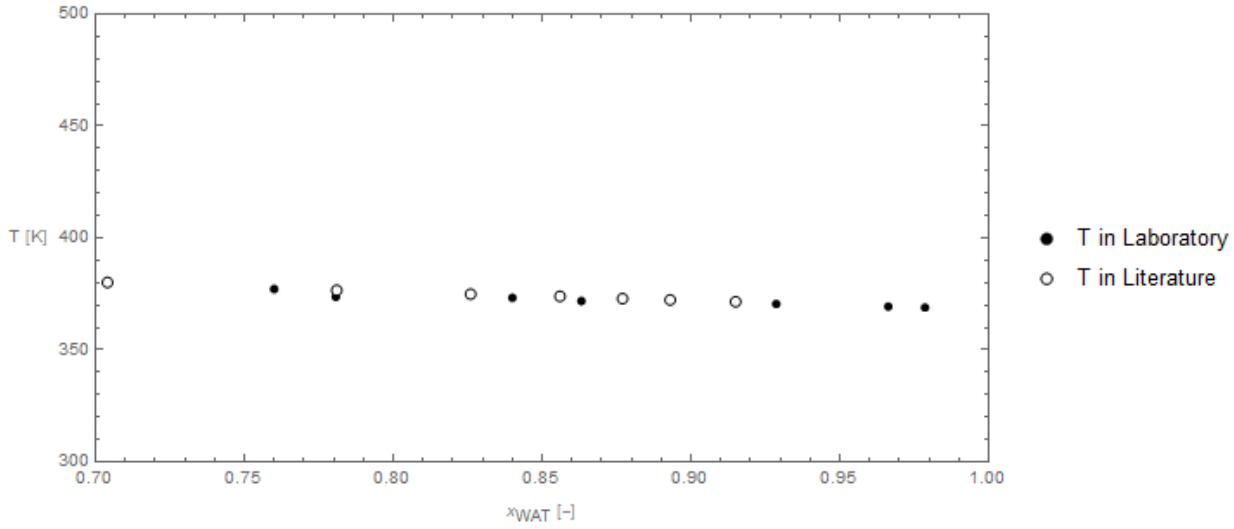

Figure 5.3: T-x data of the triethylene glycol - water mixture at $P = 850$ [mbar], from laboratory measurements and literature (see Mostafazadeh, Rahimpour, and Shariati [21])

The diagram below (figure 5.4) shows the results of the measurements on a binary mixture of 1-propanol and water (PRO-WAT) performed to validate the performance of the laboratory procedure, as well as literature data for comparison (see Udovenko, Mazanko, and Plyngeu [22], Kojima [23], and Iliuta, Thyrion, and Landauer [24]).

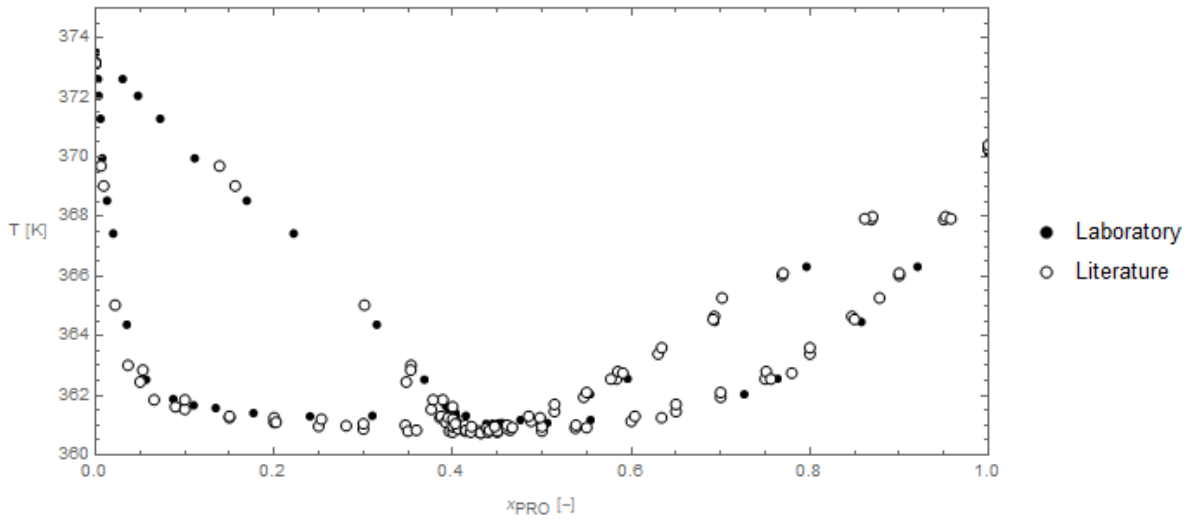

Figure 5.4: T-xy data of the 1-propanol - water mixture at $P = 1$ [atm] from experiments and literature [22], [23], [24]

As can be seen in the diagram, the azeotropic point can be estimated at a 1-propanol molar

fraction of $x_{\text{PRO}} \approx 0.43$ and a temperature of $T \approx 361$ [K], which is in agreement with literature data (see Udovenko, Mazanko, and Plyngeu [22], Kojima [23], and Iliuta, Thyrion, and Landauer [24]).

The results of the ternary system vapor-liquid equilibrium of triethylene glycol, 1-propanol and water are included in the appendix (chapter 8). Since no literature data is available for comparison, the data of the ternary systems is only used as a qualitative validation of the parameters regressed from binary system data pictured above (figures 5.1 and 5.2). The agreement of this data set with the parameters is discussed below (chapter 5.2).

5.2 Parameter Validation

After the regression had been completed, the following binary interaction parameters were determined for the two binary systems TEG-PRO and TEG-WAT.

Table 5.1: Binary interaction parameters determined in the regression

Binary Mixture	A_{ij}	A_{ji}	B_{ij}	B_{ji}	F_{ij}	F_{ji}
TEG - PRO	0.13101	0.01700	85.416	8.7777	-1.7869 E-5	1.0429 E-4
TEG - WAT	-0.46993	0.87980	-369.57	-318.97	2.8719 E-3	-4.5811 E-4

The parameters generated in the regression were first tested by comparing the boiling curve generated by the model equations with the experimental data points from the laboratory. In figure 5.5, the diagram shows the experimental data for the binary system TEG-PRO as well as the boiling curve resulting from the generated NRTL parameters. Visually, the model generated boiling curve and the data points show parity. To quantify the agreement of the data and the model, the mean relative deviation and the root mean square relative deviation $RMSRD_T$ of the pictured temperature data and model curve were determined.

The mean relative deviation of the system TEG-PRO was determined to be $\Delta T_{\text{Rel}} = 0.0030584$ Calculated according to equation (4.11), the root mean square relative deviation for the system TEG-PRO was determined to be $RMSRD_T = 0.0035886$.

The boiling curve calculated with the determined NRTL parameters for the TEG-WAT system also showed visually promising results, as pictured in figure 5.6. As for the previous system, mean relative deviation and the root mean square relative deviation of the temperature data and the model curve were determined. The mean relative deviation of the temperature amounts to $\Delta T_{\text{Rel}} = 0.0026942$. The root mean square relative deviation is slightly larger with

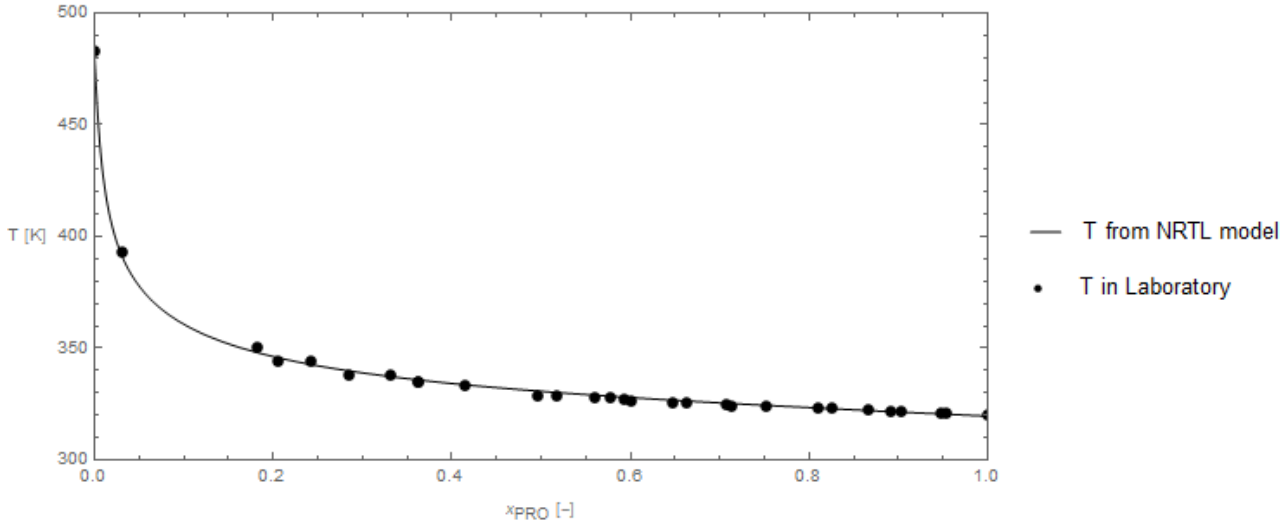

Figure 5.5: T-x data of the triethylene glycol - 1-propanol mixture at $P = 100$ [mbar] and boiling curve calculated using the determined NRTL parameters

$RMSRD_T = 0.0038247$. Overall, the regressed NRTL parameters boiling curves show high parity with the experimental temperature data.

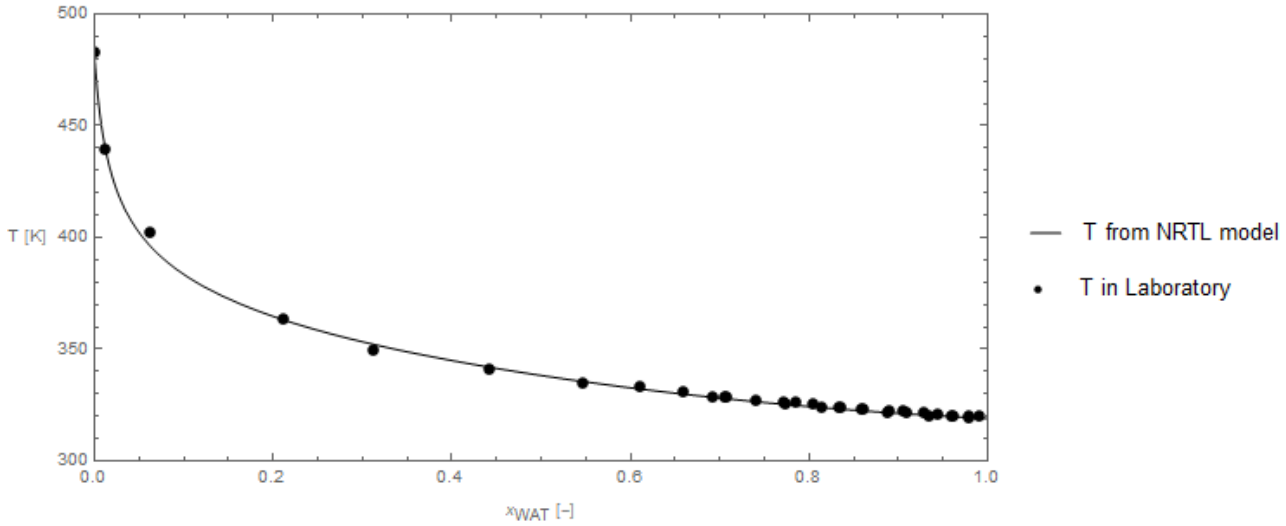

Figure 5.6: T-x data of the triethylene glycol - water mixture at $P = 100$ [mbar] and boiling curve calculated using the determined NRTL parameters

The root mean square deviations of the pressures calculated during the regression show larger values ($RMSRD_P = 0.057394$ for TEG-PRO and $RMSRD_P = 0.0563544$ for TEG-WAT). This complication arises due to the use of isobaric data sets and due to deviations introduced by the Antoine parameters, for the calculation of the vapor pressures of the pure substances at a given temperature. Since the problem arises from calculating pressure from temperature this

effect cancels out when the so determined pressure is taken to calculate temperature again, thus resulting in the low values of $RMSRD_T$ during the comparison of temperature data described above.

In the diagram of figure 5.7, the T-x data for the TEG-WAT binary system at $P = 850$[mbar], together with literature data [21] is pictured. Also, a boiling curve calculated using the generated NRTL parameters has been drawn. The model seems capable to describe this data at a different pressure adequately.

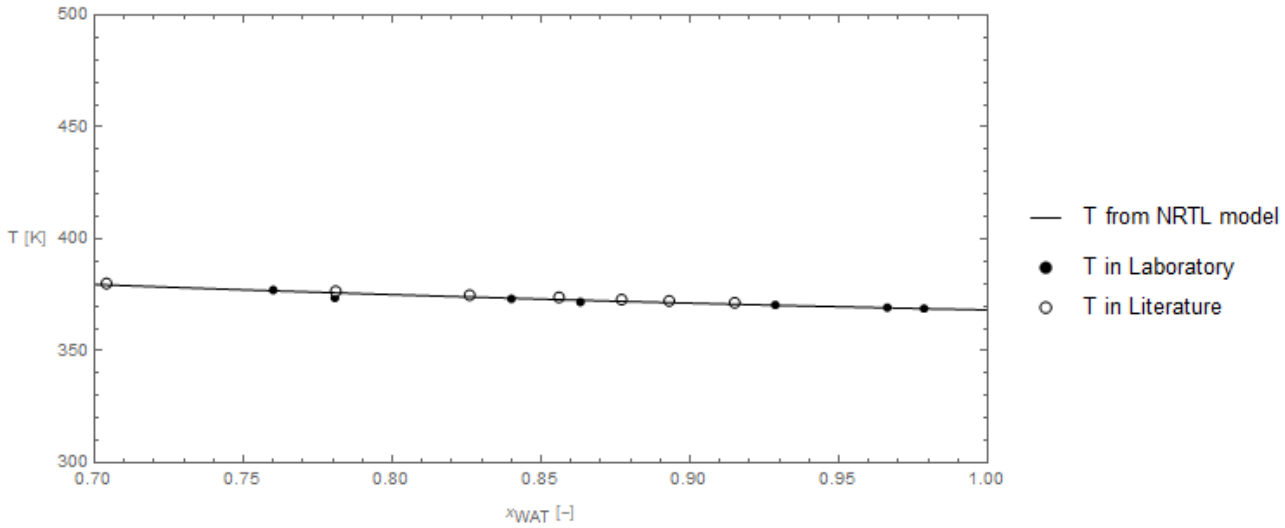

Figure 5.7: T-x data of the triethylene glycol - water mixture at $P = 850$ [mbar] from experiments and literature (see Mostafazadeh, Rahimpour, and Shariati [21]) and boiling curve calculated using the determined NRTL parameters

As explained above (chapter 4.4) the NRTL parameters were not only fitted to vapor-liquid equilibrium data, but also to data of activity coefficients at infinite dilution γ^{∞}. The data for this was taken from literature (see Gmehling [6] for TEG-PRO and Gmehling [7] for TEG-WAT). It is important to note that in both cases γ^{∞} data only for the infinite dilution of water or 1-propanol in triethylene glycol as solvent was used.

Figure 5.8 shows the infinite dilution activity coefficient data and the curve generated by the model parameters. Visually, the diagram shows acceptable agreement of the data and model, however, because of the sparse data a definitive call can not be made. The root mean square relative deviation for this data is $RMSRD_{\gamma^{\infty}} = 0.017015$.

Figure 5.9 shows the agreement of the infinite dilution activity coefficient data for the binary system TEG-WAT with the NRTL model parameter generated curve. Visually, the agreement of the individual data points as well as the overall trend of the curve seems satisfactory. The root mean

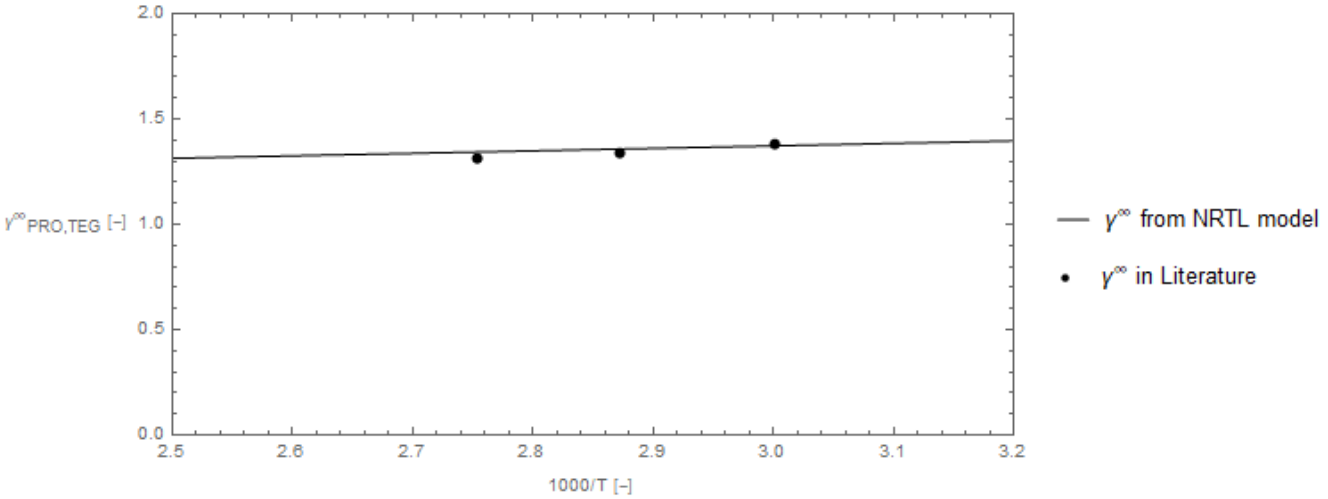

Figure 5.8: Infinite dilution activity coefficients γ^{∞} data from literature (Gmehling [6]), together with the NRTL model calculated γ^{∞} over temperature $\frac{1000}{T}$ curve

square relative deviation of the infinite dilution activity coefficients is $RMSRD_{\gamma^{\infty}} = 0.0063251$.

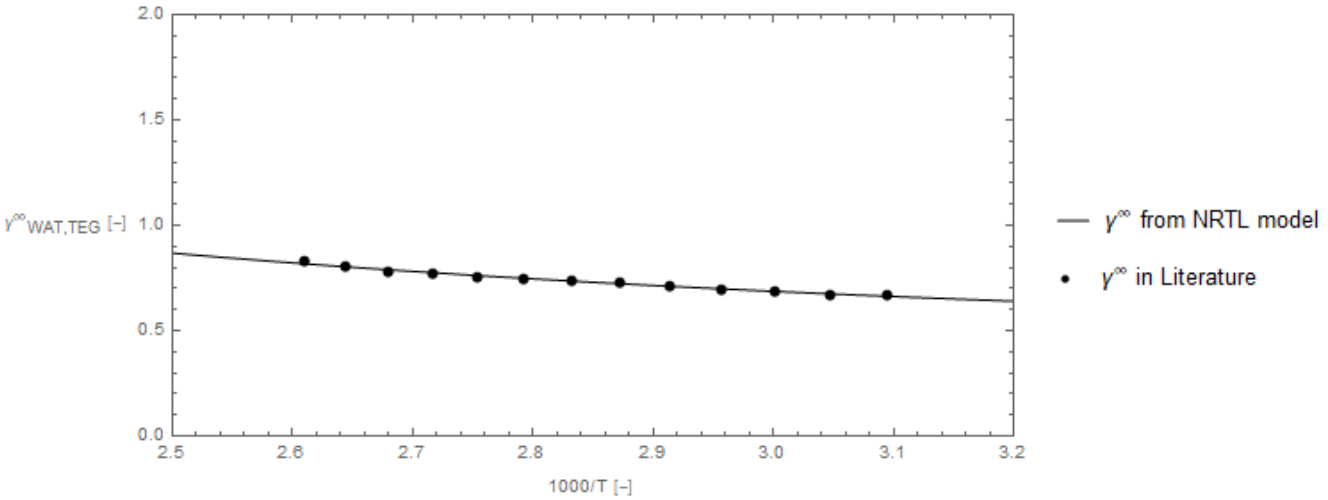

Figure 5.9: Infinite dilution activity coefficients γ^{∞} data from literature (Gmehling [7]), together with the NRTL model calculated γ^{∞} over temperature $\frac{1000}{T}$ curve

These values of $RMSRD_{\gamma^{\infty}}$ can be seen as an affirmation that the fit is well suited, as in literature a value of up to $RMSRD_{\gamma^{\infty}} \approx 5\%$ is seen as acceptable (see [8]).

Another qualifying property for the parameter set should be its ability to produce a coherent course of the activity coefficients over the molar fraction range. Therefore, these curves were plotted over the whole molar fraction range. Some requirements for the so generated curves exist in literature. The lines of γ^{∞} should normally have a steady curvature toward the region of infinite dilution. However for isobaric data sets, some minima or maxima are not uncommon in mixtures

with a high range of boiling points (as were studied here) due to the dependency of the activity coefficients on the temperature. Also a situation where the infinite dilution activity coefficients are not both below or both above 1 is unusual. Also, activity coefficients below 0.1 are an indication of chemical reactions taking place, which have to be accounted for separately. [8]

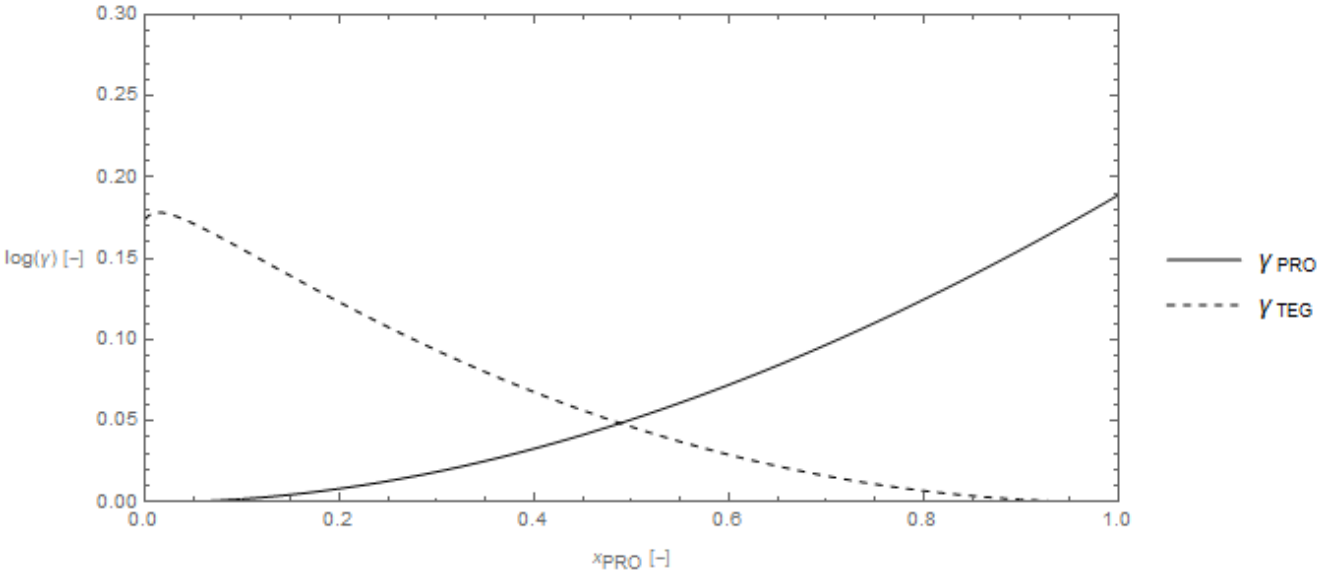

Figure 5.10: Activity coefficient curves generated with NRTL parameters of the TEG-PRO system

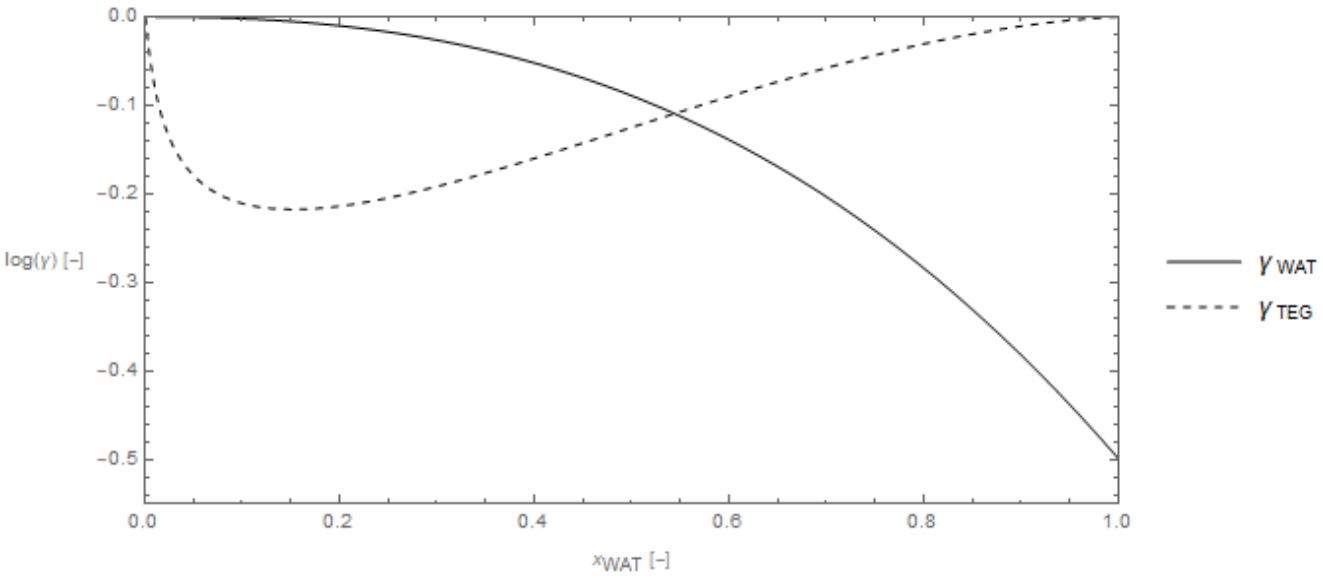

Figure 5.11: Activity coefficient curves generated with NRTL parameters of the TEG-WAT system

As visible in the two figures 5.10 and 5.11, the NRTL parameters do not produce activity coefficients in conflict with the aforementioned criteria. The activity coefficients are constantly above

$\gamma_i = 1$ ($\log_{10}(\gamma_i) = 0$) for the TEG-PRO system, and below $\gamma_i = 1$ ($\log_{10}(\gamma_i) = 0$) for the TEG-WAT system. The γ_{TEG} curves in both instances present local maxima, which is to be expected, as the VLE data used did stem from isobaric data sets. Also, none of the activity coefficients falls below the $\gamma_i = 0.1$ ($\log_{10}(\gamma_i) = -1$) level, indicating no chemical reactions, as expected.

The parameters generated seem reliable in reproducing the data they were generated with, as well as computing T-x data at moderately different pressures. To test the reliability of the NRTL model and its parameters regarding the behaviour of a ternary system, the last pair of binary parameters for the system PRO-WAT is needed. These parameters were taken from literature (see Zhang et al. [12]) and given in table 5.2, which contains the whole parameter set used for further calculations.

Table 5.2: Binary interaction parameters and non-randomness parameters used for further evaluations

Binary Mixture	α_{ij}	A_{ij}	A_{ji}	B_{ij}	B_{ji}	F_{ij}	F_{ji}
PRO - WAT	0.47	-1.7387	3.2932	799.35	-238.29	0	0
TEG - PRO	0.30	0.13101	0.01700	85.416	8.7777	-1.7869 E-5	1.0429 E-4
TEG - WAT	0.30	-0.46993	0.87980	-369.57	-318.97	2.8719 E-3	-4.5811 E-4

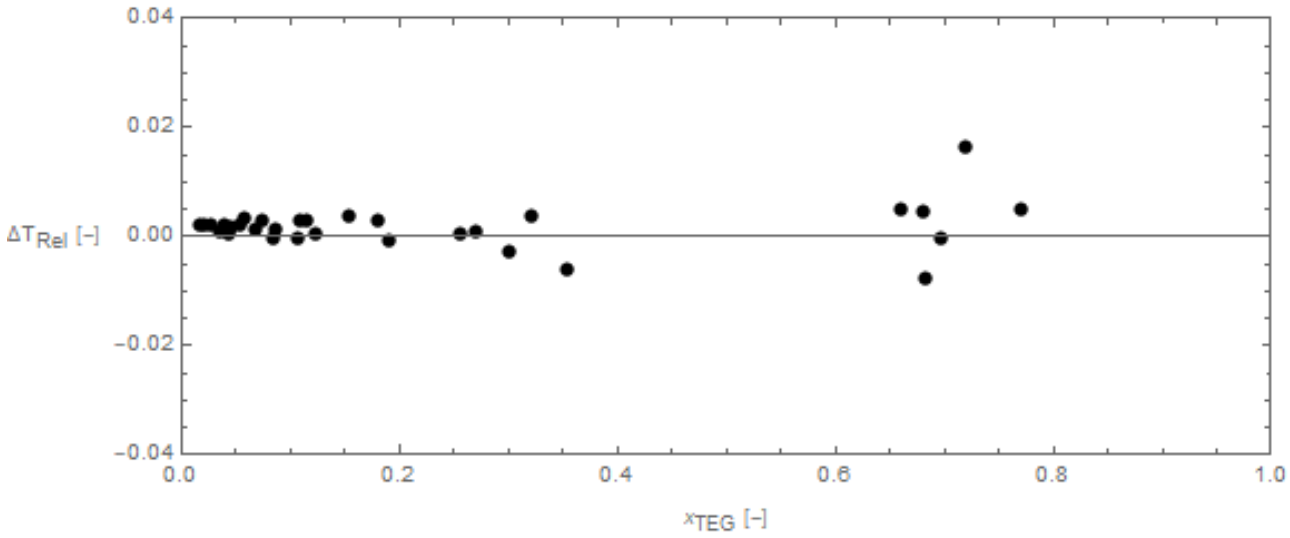

Figure 5.12: Relative deviation of the temperature data measured for the ternary system TEG-PRO-WAT

As visible in figure 5.12, where the relative deviations of the model generated vapor pressure plane and the temperature data from the laboratory is visualised, the NRTL model is capable to reproduce the behaviour of the ternary system to a certain extend. Some deviations are still visible,

again with a trend of the deviations increasing with the molar fraction of triethylene glycol x_{TEG} and therefore the temperature T. The root mean square relative deviation $RMSRD_T = 0.0042279$ also points to a high parity of the NRTL parameter generated temperature and the measured data.

5.3 Entrainer Evaluation

With the generated NRTL model parameter set, a more comprehensive review of the entrainer substance is possible. As explained in chapter 2.1, multiple criteria should be considered. Triethylene glycol was picked over ethylene glycol and diethylene glycol since it does not present with the complications of toxicity and hazardous substance handling requirements as the others do [13], [14], [25]. Additionally, for ethylene glycol, as for glycerol, a set of NRTL parameters, as well as an evaluation concerning their feasibility as entrainers is already available in literature [12], [4]. This now allows for a detailed comparison of the entrainers. In figure 5.13 the univolatility line $\alpha_{\mathrm{PRO,WAT}} = 1$ as well as the isovolatility lines of $\alpha_{\mathrm{PRO,WAT}} = \{0.5;\ 2.0;\ 4.0\}$, as calculated using equation (2.3), are depicted.

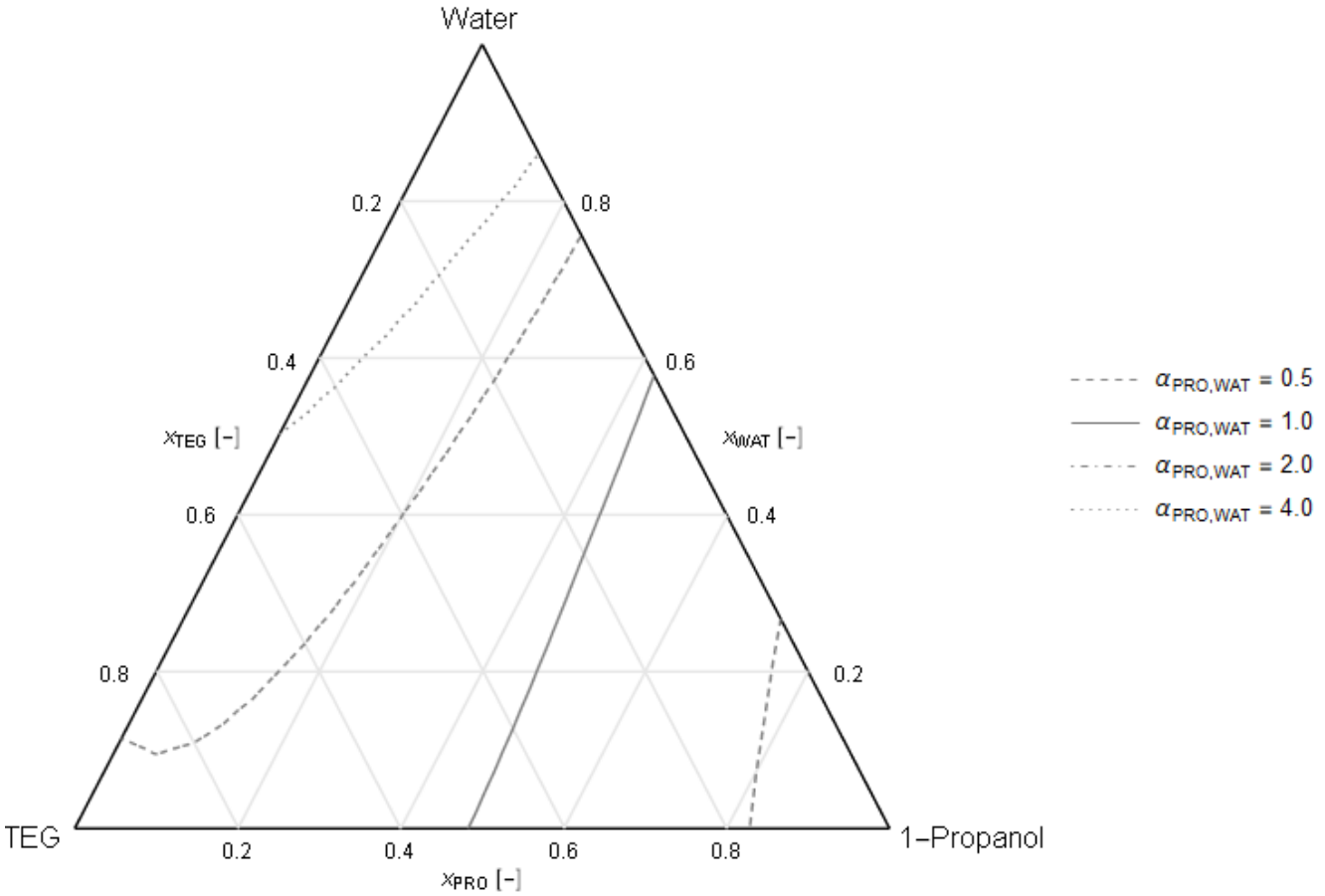

Figure 5.13: Isovolatility lines in the ternary diagram of the system TEG-PRO-WAT, on molar fraction basis

As visible in the diagram (figure 5.13), the isovolatility curves show a broad region of relatively low deviation of the relative volatility from unity, as indicated by the distance in between the isovolatility lines of $\alpha_{\mathrm{PRO,WAT}} = 0.5$ and $\alpha_{\mathrm{PRO,WAT}} = 2.0$. Near the vertices of pure water and pure 1-propanol, the deviations from unity increase. From the intersect of the univolatility line $\alpha_{\mathrm{PRO,WAT}} = 1$ with the line of water free mixture $x_{\mathrm{WAT}} = 0$, the minimal entrainer mole fraction $x_{\mathrm{TEG,min}} = 0.515$ can be determined. This value marks the entrainer amount needed to eliminate the azeotropic behaviour of the 1-propanol - water subsystem in the ternary mixture and corresponds to a minimal entrainer mass fraction of $w_{\mathrm{TEG,min}} = 0.727$. Compared to the minimal entrainer mass fraction of glycerol, calculated from NRTL parameters reported by Zhang et al. [12] $w_{\mathrm{GLY,min}} = 0.505$, and the minimal entrainer mass fraction for ethylene glycol as reported by Pla-Franco et al. [4] $w_{\mathrm{EG,min}} = 0.588$, the needed mass fraction of triethylene glycol to eliminate the azeotropic behaviour is much higher. This finding is also in agreement with the screening results concerning selectivity, where glycerol delivers the best results and ethylene glycol performed better than triethylene glycol.

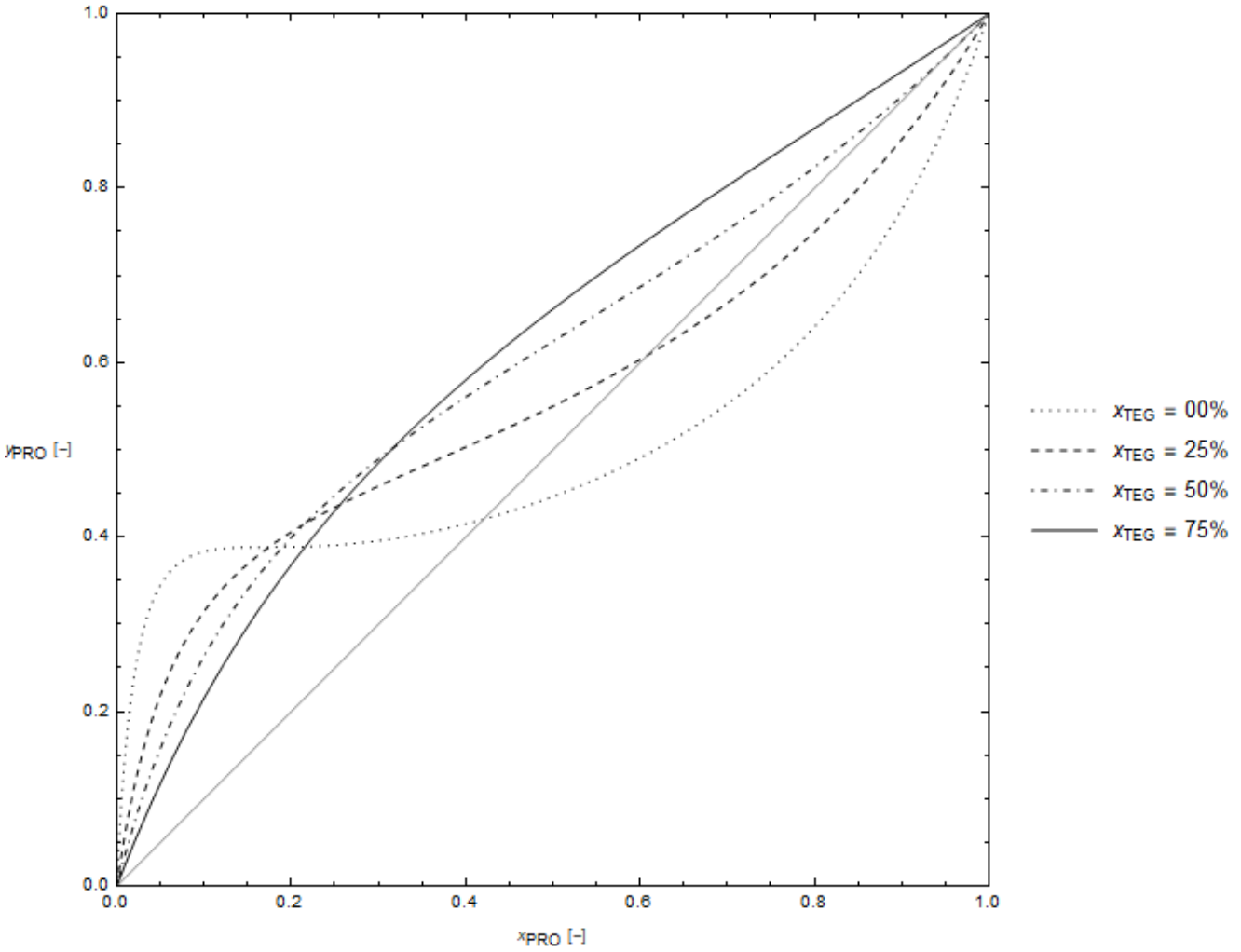

Figure 5.14: Pseudo binary McCabe-Thiele diagram of 1-propanol - water mixtures with constant triethylene glycol molar fractions

In figure 5.14, a pseudo-binary McCabe-Thiele diagram is depicted, as plotted using the parameters stated in table 5.2, showing the impact of added triethylene glycol on the azeotropic behaviour of 1-propanol and water. The diagram also shows, what can already be observed in the ternary diagrams (figures 5.13 and 5.15), that the addition of triethylene glycol to the equivalent of a molar fraction of $x_{\mathrm{TEG}} = 0.50$ is almost enough to eliminate the azeotrope, while at $x_{\mathrm{TEG}} = 0.75$ the azeotropic behaviour is no longer existent.

The residue curves of the ternary system were also plotted, as visible in figure 5.15, and behave as expected for a ternary system with one low boiling binary azeotrope. They show behaviour comparable to that reported by Pla-Franco et al. [4] for the ternary system of ethylene glycol, 1-propanol and water.

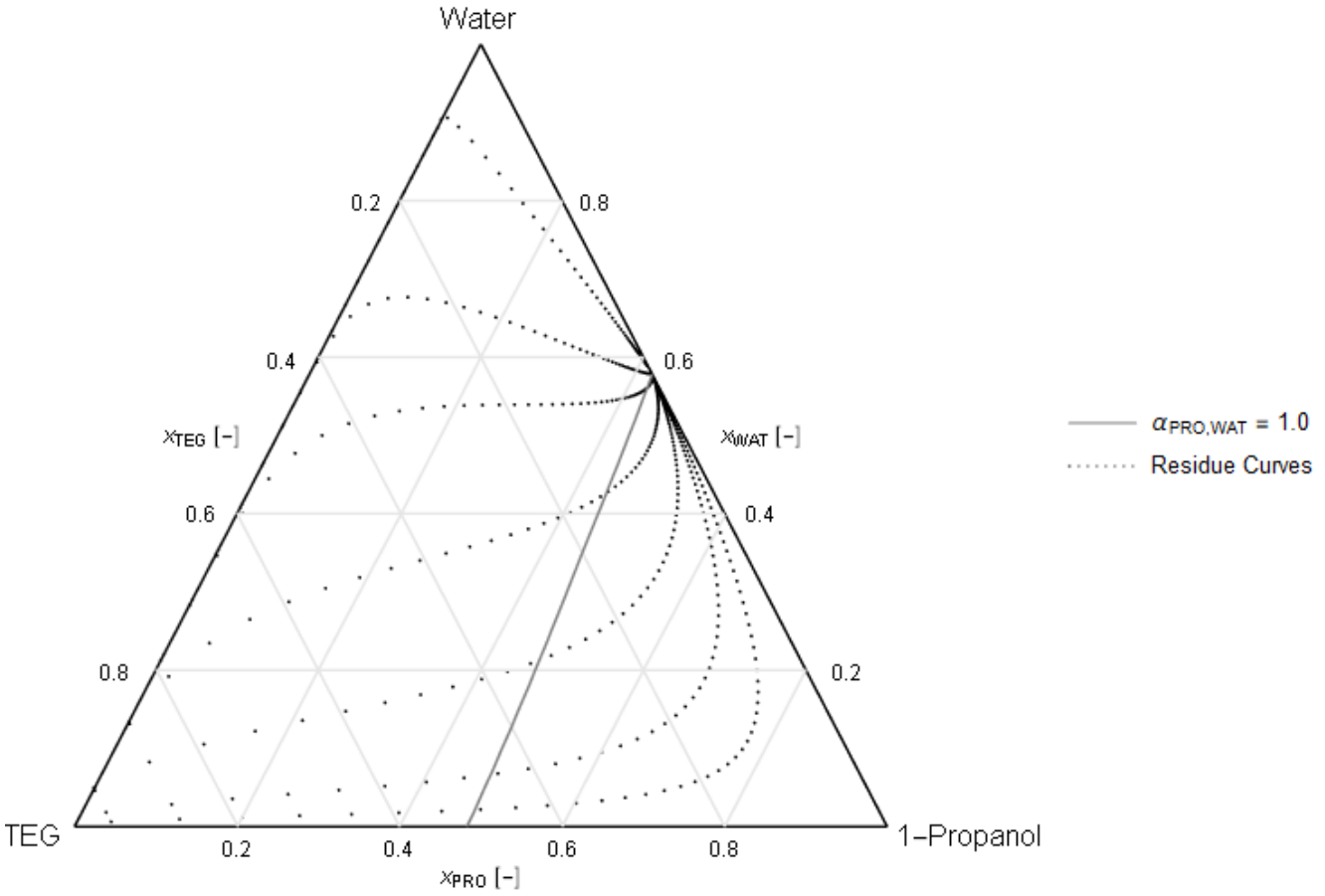

Figure 5.15: Residue curves in the ternary diagram of the system TEG-PRO-WAT, on molar fraction basis, as well as univolatility line

All in all, it can be stated, that the data generated from NRTL parameters show satisfying parity with experimental data of the ternary system, and the behaviour described by the NRTL model is suitable for a usage of triethylene glycol as entrainer in an extractive distillation of the 1-propanol water mixture. While triethylene glycol seemingly requires a higher minimum mass fraction $w_{\mathrm{TEG,min}}$ than glycerol and ethylene glycol, the benefits of the reduced risk in handling and lower viscosity of triethylene glycol [16] may outweigh the performance edge of toxic ethylene glycol and highly viscous glycerol [15]. A mixture of triethylene glycol and glycerol may also be considered favorable to potentially combine the high separation efficiency of glycerol with the lower viscosity of triethylene glycol.

6 Summary and Outlook

The aim of this thesis was to generate a vapor-liquid equilibrium data set for the previously non investigated behaviour of a 1-propanol and triethylene glycol mixture, as well as finding a descriptive NRTL model parameter set, and a first evaluation of the feasibility of triethylene glycol as an entrainer for extractive distillation of 1-propanol and water mixtures.

First, a set of vapor liquid equilibrium measurements in an isobaric equilibrium still was performed. Vapor and liquid phase samples were taken from the system in its equilibrium state and analysed using gas chromatography analysis, Karl-Fischer titration and density measurements. After a vapor-liquid equilibrium data set comprising $T - x$ data of the binary mixtures of all relevant substances - triethylene glycol, 1-propanol and water - had been assembled, this data was validated with existing literature data, when possible. After the parity of the data set and literature data had been found satisfactory, the parameters for the NRTL model for Gibbs excess enthalpy were determined.

For this purpose, then, a routine for the minimisation of an objective function by variation of the model parameters was devised. This objective function was formulated to include the weighted errors of the model predicted data compared to the experimental and literature data. The data used in this routine were not only vapor-liquid equilibrium data, but also infinite dilution activity coefficient data. The potential inclusion of excess enthalpy data in the objective function was enabled but, due to lacking availability of this data, it was not taken into account in this parameter regression.

The generated NRTL parameters were tested by again comparing them to the data set they were generated from, as well as holding them up to general criteria for activity coefficient behaviour. After these comparisons were satisfactory, they were compared to ternary vapor-liquid equilibrium data measured in the laboratory for this purpose. Since the generated NRTL parameters not only described the binary mixture data very well and held up to the criteria formulated for the behaviour of activity coefficients in binary mixtures, but they were also able to describe the behaviour of the ternary system within a certain deviation range. The NRTL parameters were found to be representative enough to allow judgement on the feasibility of the devised extractive distillation process.

Therefore, ternary mixture diagrams were plotted using the regressed parameters, picturing iso-volatility and residue curves, as well as pseudo binary McCabe-Thiele diagrams, showing that the azeotropic behaviour of the 1-propanol water mixture can be eliminated with a minimum molar

fraction of triethylene glycol of $x_{\mathrm{TEG,min}} = 0.515$, which corresponds to a minimum mass fraction of $w_{\mathrm{TEG,min}} = 0.727$. While this required mass fraction is higher than that of other entrainer candidates, the process is still feasible and the beneficial general properties of triethylene glycol such as low toxicity compared to ethylene glycol and lower viscosity compared to glycerol as well as the process specific properties of triethylene glycol potentially balance out the perceived thermodynamic inferiority.

For further investigation, multiple points remain. If deemed necessary, the NRTL parameter set may be further refined by including excess enthalpy data in the parameter determination. Also the superiority of isothermal vapor-liquid equilibrium data over isobaric data in parameter regressions shall be mentioned. For the accurate assessment of the choice of triethylene glycol as entrainer in an extractive distillation process, deciding process parameters like feed composition and target purities of the products would be necessary, together with a series of laboratory distillation experiments. Finally, estimating investment and operating costs based on comprehensive process simulations should enable a more robust and reliable comparison with other potential candidates.

7 Bibliography

[1] Shota Atsumi and James C Liao. "Directed evolution of Methanococcus jannaschii citramalate synthase for biosynthesis of 1-propanol and 1-butanol by Escherichia coli". In: *Applied and environmental microbiology* 74.24 (2008), pp. 7802–7808.

[2] Mengpan Wang et al. "Catalytic transformation of glycerol to 1-propanol by combining zirconium phosphate and supported Ru catalysts". In: *RSC Adv.* 6 (35 2016), pp. 29769–29778. DOI: 10.1039/C6RA02682F. URL: http://dx.doi.org/10.1039/C6RA02682F.

[3] Ruihan Luo et al. "Effect of Tungsten Modification on Zirconium Phosphate-Supported Pt Catalyst for Selective Hydrogenolysis of Glycerol to 1-Propanol". In: *Energy & Fuels* 34.7 (2020), pp. 8707–8717. DOI: 10.1021/acs.energyfuels.0c00645. URL: https://doi.org/10.1021/acs.energyfuels.0c00645.

[4] Jordi Pla-Franco et al. "Approach to the 1-propanol dehydration using an extractive distillation process with ethylene glycol". In: *Chemical Engineering and Processing: Process Intensification* 91 (2015), pp. 121–129. ISSN: 0255-2701. DOI: https://doi.org/10.1016/j.cep.2015.03.007. URL: https://www.sciencedirect.com/science/article/pii/S0255270115000537.

[5] Vincent Gerbaud et al. "Review of extractive distillation. Process design, operation, optimization and control". In: *Chemical Engineering Research and Design* 141 (2019), pp. 229–271. ISSN: 0263-8762. DOI: https://doi.org/10.1016/j.cherd.2018.09.020. URL: https://www.sciencedirect.com/science/article/pii/S0263876218304660.

[6] Jürgen Gmehling. *Chemistry data series : 9, Activity coefficients at infinite dilution, 5 : C1 - C16 / J. Gmehling ...* eng. Dechema, Deutsche Gesellschaft für Chemisches Apparatewesen, Chemische Technik und Biotechnologie, 2007. ISBN: 9783897460904.

[7] Jürgen Gmehling, ed. *1-Propanol-Water Activity Coefficients at Infinite Dilution: Datasheet from "Dortmund Data Bank (DDB) - Thermophysical Properties Edition 2014" in SpringerMaterials.* accessed 10.04.2022. URL: https://materials.springer.com/thermophysical/docs/act_c140c174.

[8] Jürgen Gmehling et al. *Chemical thermodynamics for process simulation.* eng. Second, completely revised and enlarged edition. 2019. ISBN: 9783527343256.

[9] Henri Renon and John M Prausnitz. "Local compositions in thermodynamic excess functions for liquid mixtures". In: *AIChE journal* 14.1 (1968), pp. 135–144.

[10] Yasar Demirel. "Calculation of infinite dilution activity coefficients by the NRTL and UNIQUAC models". In: *The Canadian Journal of Chemical Engineering* 68 (Aug. 1990), pp. 697–701. DOI: 10.1002/cjce.5450680424.

[11] Qiang Yang et al. "Potential explosion hazards associated with the autocatalytic thermal decomposition of dimethyl sulfoxide and its mixtures". In: *Organic Process Research & Development* 24.6 (2020), pp. 916–939.

[12] Lianzhong Zhang et al. "Experimental Measurement and Modeling of Vapor-Liquid Equilibrium for the Ternary System Water + 1-Propanol + Glycerol". In: *Journal of Chemical & Engineering Data* 61.4 (2016), pp. 1637–1644. DOI: 10.1021/acs.jced.5b01015. URL: https://doi.org/10.1021/acs.jced.5b01015.

[13] *European Chemicals Agency: Substance Infocard Ethane-1,2-diol*. accessed 18.10.2022. URL: https://echa.europa.eu/de/substance-information/-/substanceinfo/100.003.159.

[14] *European Chemicals Agency: Substance Infocard 2,2'-oxydiethanol*. accessed 18.10.2022. URL: https://echa.europa.eu/de/substance-information/-/substanceinfo/100.003.521.

[15] Abel G.M. Ferreira et al. "The viscosity of glycerol". In: *The Journal of Chemical Thermodynamics* 113 (2017), pp. 162–182. ISSN: 0021-9614. DOI: https://doi.org/10.1016/j.jct.2017.05.042. URL: https://www.sciencedirect.com/science/article/pii/S0021961417301817.

[16] Zhenhua Guo et al. "Liquid viscosities, excess properties, and viscous flow thermodynamics of triethylene glycol+ water mixtures at T=(298.15, 303.15, 308.15, 313.15, and 318.15) K". In: *Journal of Molecular Liquids* 165 (2012), pp. 27–31.

[17] Gerhard Spruk. "Aufbau einer Laborübung zur Dampf- Flüssig- Gleichgewichtsmessung (Vapor- Liquid- Equilibrium)". MA thesis. Graz University of Technology, 2009.

[18] *NIST Chemistry Webbook, SRD 69: Water*. accessed 12.10.2022. URL: https://webbook.nist.gov/cgi/cbook.cgi?ID=C7732185&Units=SI&Mask=4&Type=ANTOINE&Plot=on#ANTOINE.

[19] *NIST Chemistry Webbook, SRD 69: 1-Propanol*. accessed 12.10.2022. URL: https://webbook.nist.gov/cgi/cbook.cgi?ID=C71238&Units=SI&Mask=4&Type=ANTOINE&Plot=on#ANTOINE.

[20] *NIST Chemistry Webbook, SRD 69: Triethylene glycol*. accessed 12.10.2022. URL: https://webbook.nist.gov/cgi/cbook.cgi?ID=C112276&Units=SI&Mask=4&Type=ANTOINE&Plot=on#ANTOINE.

[21] Ali Khosravanipour Mostafazadeh, Mohammad Reza Rahimpour, and Alireza Shariati. "Vapor-Liquid Equilibria of Water + Triethylene Glycol (TEG) and Water + TEG + Toluene at 85 kPa". In: *Journal of Chemical & Engineering Data* 54.3 (2009), pp. 876–881. DOI: 10.1021/je800675u. URL: https://doi.org/10.1021/je800675u.

[22] VV Udovenko, TF Mazanko, and V Ya Plyngeu. *Liquid-vapor equilibrium in normal propyl alcohol-water and normal propyl alcohol benzene systems*. 1972.

[23] K Kojima. "Determination of vapor-liquid equilibrium from boiling point curve". In: *Kagaku Kogaku* 32 (1968), pp. 149–153.

[24] Maria C Iliuta, Fernand C Thyrion, and Ortansa M Landauer. "Effect of calcium chloride on the isobaric vapor- liquid equilibrium of 1-propanol+ water". In: *Journal of Chemical & Engineering Data* 41.3 (1996), pp. 402–408.

[25] *European Chemicals Agency: Substance Infocard 2,2'-(ethylenedioxy)diethanol*. accessed 18.10.2022. URL: https://echa.europa.eu/de/substance-information/-/substanceinfo/100.003.594.

8 Appendix

Table 8.1: Ternary VLE data generated in laboratory experiments using the VLE602 equilibrium still

Sample ID	T [K]	P [mbar]	w^I_{TEG}	w^I_{PRO}	w^I_{WAT}	σ_T	σ_P
Tern0.3_1.01	365.27	1010.93	0.283	0.616	0.100	0.10219	1.6335
Tern0.3_1.02	363.30	1010.44	0.264	0.554	0.182	0.05738	1.8960
Tern0.3_1.03	362.35	1011.27	0.189	0.427	0.384	0.03660	1.6267
Tern0.3_2.01	362.54	1012.54	0.183	0.298	0.519	0.09885	1.3502
Tern0.3_2.02	362.54	1009.31	0.140	0.318	0.541	0.08933	2.4693
Tern0.3_2.03	362.97	1011.98	0.127	0.211	0.662	0.07227	2.0675
Tern0.3_2.04	363.26	1012.83	0.105	0.179	0.717	0.01551	2.4609
Tern0.5_1.01	367.04	1011.06	0.435	0.407	0.167	0.21744	1.3163
Tern0.5_1.02	364.61	1009.98	0.391	0.316	0.244	0.16540	1.9121
Tern0.5_1.03	364.03	1011.90	0.350	0.302	0.359	0.07262	1.0338
Tern0.5_2.01	363.76	1010.86	0.312	0.256	0.439	0.07073	1.0445
Tern0.5_2.02	363.84	1011.47	0.266	0.219	0.514	0.07977	1.6206
Tern0.5_2.03	364.09	1011.47	0.244	0.170	0.578	0.00000	1.8599
Tern0.5_2.04	364.66	1011.80	0.246	0.149	0.698	0.01932	1.9890
Tern0.7_1.01	368.08	1010.44	0.555	0.218	0.238	0.68384	1.7588
Tern0.7_1.02	367.28	1011.75	0.577	0.201	0.235	0.53140	1.4889
Tern0.7_1.03	366.69	1012.02	0.415	0.148	0.341	0.11225	1.2477
Tern0.7_1.04	366.39	1009.72	0.484	0.178	0.422	0.10906	2.1430
Tern0.7_1.05	366.33	1011.94	0.365	0.126	0.512	0.02799	1.3477
Tern0.7_1.06	366.82	1012.08	0.318	0.103	0.593	0.07744	1.5984
Tern0.8_1.01	407.64	1012.65	0.886	0.103	0.010	0.29331	0.5447
Tern0.8_1.02	410.43	1016.66	0.920	0.066	0.013	0.43014	0.5700
Tern0.8_1.03	400.02	1012.64	0.892	0.082	0.026	0.48926	0.6026
Tern0.8_1.04	398.91	1012.63	0.891	0.077	0.032	0.38816	0.5987
Tern0.8_1.05	398.00	1012.64	0.912	0.054	0.035	0.86087	0.5711
Tern0.8_1.06	403.53	1012.57	0.921	0.044	0.035	0.93034	0.6294
Tern0.8_1.10	377.69	1012.45	0.792	0.048	0.160	0.78393	0.7110
Tern0.8_1.11	380.66	1012.56	0.774	0.041	0.185	0.27960	0.7613
Tern0.8_1.12	377.45	1012.38	0.760	0.040	0.200	0.46862	0.7516
Tern0.8_1.13	377.16	1012.13	0.732	0.042	0.226	0.27075	0.8857
Tern0.8_1.14	376.90	1012.28	0.721	0.038	0.242	0.35099	0.8442

Table 8.2: Material properties used during calculations

Property	Symbol	Unit	Triethylene glycol	1-Propanol	Water
Molar Mass	MM	[g/mol]	150.17	60.0952	18.01528
Antoine Parameter	A	[$\log_{10}$/bar/K]	6.75680	4.87601	5.08354
Antoine Parameter	B	[$\log_{10}$/bar/K]	3715.222	1441.629	1663.125
Antoine Parameter	C	[$\log_{10}$/bar/K]	-1.299	-74.299	-45.622